PNL-5278
UC-41

6A

Effects of Particle Size and Velocity on Burial Depth of Airborne Particles in Glass Fiber Filters

D. P. Higby

November 1984

Prepared for the U.S. Department of Energy
under Contract DE-AC06-76RLO 1830

Pacific Northwest Laboratory
Operated for the U.S. Department of Energy
by Battelle Memorial Institute

Battelle

PNL-5278

DISCLAIMER

PACIFIC NORTHWEST LABORATORY
operated by
BATTELLE
for the
UNITED STATES DEPARTMENT OF ENERGY
under Contract DE-AC06-76RLO 1830

Printed in the United States of America
Available from
National Technical Information Service
United States Department of Commerce
5285 Port Royal Road
Springfield, Virginia 22161

NTIS Price Codes
Microfiche A01

Printed Copy

Pages	Price Codes
001-025	A02
026-050	A03
051-075	A04
076-100	A05
101-125	A06
126-150	A07
151-175	A08
176-200	A09
201-225	A010
226-250	A011
251-275	A012
276-300	A013

PNL-5278
UC-41

EFFECTS OF PARTICLE SIZE AND VELOCITY ON BURIAL DEPTH OF AIRBORNE PARTICLES IN GLASS FIBER FILTERS

D. P. Higby

November 1984

This document was submitted as a thesis in partial fulfillment of the requirements for the degree of Master of Science in Radiological Sciences for the University of Washington.

Prepared for
U. S. Department of Energy
under Contract DE-AC06-76RLO 1830

Pacific Northwest Laboratory
Richland, Washington 99352

SUMMARY

Air sampling for particulate radioactive material involves collecting airborne particles on a filter and then determining the amount of radioactivity collected per unit volume of air drawn through the filter. The amount of radioactivity collected is frequently determined by directly measuring the radiation emitted from the particles collected on the filter. Counting losses caused by the particle becoming buried in the filter matrix may cause concentrations of airborne particulate radioactive materials to be underestimated by as much as 50%. Furthermore, the dose calculation for inhaled radionuclides will also be affected.

The present study was designed to evaluate the extent to which particle size and sampling velocity influence burial depth in glass-fiber filters. Aerosols of high-fired $^{239}PuO_2$ were collected at various sampling velocities on glass-fiber filters. The fraction of alpha counts lost due to burial was determined as the ratio of activity detected by direct alpha count to the quantity determined by photon spectrometry.

The results show that burial of airborne particles collected on glass-fiber filters appears to be a weak function of sampling velocity and particle size. Counting losses ranged from 0 to 25%. A correction that assumes losses of 10 to 15% would ensure that the concentration of airborne alpha-emitting radionuclides would not be underestimated when glass-fiber filters are used.

CONTENTS

LIST OF FIGURES

LIST OF FIGURES (continued)

LIST OF TABLES

ACKNOWLEDGEMENTS

The author wishes to express sincere appreciation to the members of his supervisory committee for their assistance in the preparation of this manuscript, and to the U.S. Department of Energy, Office of Nuclear Safety, for providing the support which made this work possible. Special thanks are due to my advisor, Professor Ronald L. Kathren and to my research supervisor, Mr. Jofu Mishima for their assistance and strategic prodding during the planning stages of this work, and to Dr. W. C. Cannon for his invaluable assistance and for the use of his laboratory. Thanks also to Dr. M. A. Hoover and Dr. B. B. Boecker of the Lovelace Inhalation Toxicology Research Institute for providing the monodisperse particles used in these experiments. Dr. Henry Spitz, Mr. Earl Palmer, and Mr. Gunars Rieksts of Battelle, Pacific Northwest Laboratories provided the equipment and technical assistance for gamma spectroscopic analysis of samples. Thanks most of all to my wife, Sheila, for her patience, understanding and support.

INTRODUCTION

Air sampling for particulate radioactive material involves the collection of airborne particles on a filter with subsequent determination of the amount of radioactivity collected per unit volume of air drawn through the filter. The radioactivity collected is frequently determined by direct measurement of the radiations emitted from the particles collected on the filter. Depending on the characteristics of the filter medium, the aerosol, and sampling conditions, radioactive particles may become buried in the filter matrix during sampling. In the case of alpha-emitting radionuclides, alpha radiation emitted from particles buried in the filter material may be degraded or masked by the intervening filter material (Lioy 1983). Such burial losses may cause concentrations of airborne particulate radioactive materials (and thus dose due to inhaled radionuclides) to be underestimated by as much as 50%.

Filter performance is frequently characterized in terms of collection efficiency which is defined as the fraction of particles entering the filter that are retained by the filter. According to Hines (1983), the overall efficiency of a filter, E, is given by

$$E = 1 - \exp\left[\frac{-4\alpha\, E_T t}{\pi d_f}\right]$$

where α is the ratio of fiber volume to total volume, t is the thickness of the filter, d_f is the fiber diameter, and E_T is the total single fiber efficiency. E_T is the arithmetic sum of the single fiber efficiencies for interception, inertial impaction,

diffusion, gravitational settling, and electrostatic attraction. The theoretical single fiber efficiency for interception, E_R, is given by

$$E_R = \frac{1}{2Ku}\left[2(1+R)\ln(1+R) - (1+R) + \frac{1}{1+R}\right]$$

where Ku is the Kuwabara hydrodynamic factor. Ku depends only on α, and is given by

$$Ku = -\frac{\ln\alpha}{2} - \frac{3}{4} + \alpha - \frac{\alpha^2}{4}$$

while R is the ratio of particle size to fiber diameter. Interception is the only mechanism that does not depend on the flow velocity, U_o.

Inertial impaction depends primarily on the Stokes number, Stk, which is the ratio of particle stopping distance to fiber diameter

$$Stk = \frac{\tau U_o}{d_F}$$

where τ is the relaxation time of the particle and d_F is the fiber diameter. The single fiber efficiency for inertial impaction, E_I, is given by

$$E_I = \frac{J(Stk)}{2Ku^2}$$

where J is a constant approximately equal to 2 for $R > 0.4$. Electrostatic attraction can be extremely important but it is difficult to quantify because of lack of knowledge of the charge on fibers and particles. Diffusion is negligible for particles larger than 0.2 μm, and gravitational settling is small compared to the

other mechanisms (Hines 1983). Interception and inertial impaction are the primary collection mechanisms of interest in this study.

The dependence of collection efficiency on particle size and velocity has been well established (Stafford and Ettinger 1972, Lee and Liu 1980). In general, single fiber filtration theory predicts an aerosol size for minimum collection efficiency. This particle size is typically around 0.1 to 0.3 μm aerodynamic diameter for fiber filters. Minimum efficiency occurs at smaller aerosol sizes as velocity is increased. Experimental data have shown good agreement with theoretical predictions. It is therefore reasonable to expect a similar relationship between depth of burial, particle size, and sampling velocity.

Various investigators have reported on the depth of burial of particles collected on filters. Parnianpour (1967) found that the penetration of sub-micron particles into fibrous filters is determined primarily by the characteristics of the filter media, and secondarily by the sampling velocity. In the same study, it was found that the distribution of particles within the filter bed followed a negative exponential function. Stevens and Toureau (1963) conducted an extensive study on the effects of particle size and dust loading on the shape of alpha pulse height spectra of air sample filters. They compared alpha energy spectra from several types of filters and found that, in general, glass-fiber filters tend to be surface loading, thereby reducing the need (in their opinion) for correction for burial losses. More frequently, the percent of alpha particles absorbed by the filter medium is

reported. Alercio and Harley (1952) found that 30% of the alpha particles emitted from uranium compounds (U_3O_8, UF_6, UO_2F_2) collected on cellulose filters were absorbed by the filter. Simons (1952) reported that 50% of plutonium alphas from particles collected on cellulose filters were absorbed, and Boback (1963) observed identical results with uranium compounds (UF_4, UO_3, U_3O_8) collected on cellulose filters. Denham (1969) reported that 40% of alpha particles from naturally occurring radon daughters were absorbed when the radioactive particles were collected on cellulose filters, although some absorption may have been due to dust loading.

In general, membrane filters are thought to be surface collectors. Lindeken and Phillips (1963) developed a method to calculate burial depth in membrane filters based on the degradation of the alpha energy spectrum of RaC', and subsequently Lindeken (1964) reported that membrane filters are essentially surface collectors at pore sizes less than 5 μm. More recently, Jonassen and Hayes (1974a,b) have demonstrated the importance of correcting for alpha absorption by membrane filters when burial depths exceed 100 μm.

The present study was designed to evaluate the extent to which particle size and sampling velocity influence the burial depth, and thus counting losses due to burial, in glass fiber filters. These two parameters have widely ranging values in occupational environments (Anderson 1963; Elder, Gonzales and Ettinger 1965; Mishima and Schwendiman 1972; Sherwood and Stevens 1965). The fraction of alpha counts lost due to burial is determined as the

ratio of activity detected by direct alpha count to the quantity determined by photon spectrometry.

METHODS AND MATERIALS

Foils bearing monodisperse particles of high-fired $^{239}PuO_2$ were obtained from Lovelace Inhalation Toxicology Research Institute (ITRI), Albuquerque, New Mexico. The particles were produced and deposited on the foils using a Lovelace Aerosol Particle Separator (LAPS). The theory and use of the LAPS to produce monodisperse particles has been well described in the literature (Kotrappa and Moss 1971, Kotrappa and Light 1972, Kotrappa et al. 1972, Raabe et al. 1975, Stober and Flachsbart 1969, Hoover and Stober 1981). The LAPS is a spiral centrifuge device that provides a continuous separation of aerosol particles down to an aerodynamic diameter (d_a) of 0.5 μm. The aerodynamic diameter of a particle is the diameter of a unit density sphere that has the same settling velocity. In the LAPS, particles are collected according to their aerodynamic size along a strip foil which lines the outer wall of the rotating spiral duct. After separation, the particle bearing foil is cut into segments bearing essentially monodisperse particles with geometric standard deviations (σ_g) less than 1.1.

The plutonium used to produce the particles was originally obtained from Oak Ridge National Laboratory. Isotopic analysis performed by Los Alamos National Laboratory showed the isotopic content (atom percent) in July, 1975, to be approximately 97% ^{239}Pu, with about 3% ^{240}Pu and less than 0.2% other Pu isotopes and ^{241}Am (Table 1). Americium 241 was separated chemically and discarded just prior to aerosol production. Concentrations of other isotopes remain essentially unchanged.

TABLE 1. Isotopic Content and Principal Radiations of Material Used for Aerosolization

Isotope	Atom %	Half-life (y)[a]	Radiation Type	Energy (keV)[a]	Abundance (%)[a]
^{238}Pu	0.014	87.75	α	5499.21	71.6
^{239}Pu	96.91	24,131	α	5155.4	73.3
			L X-ray	13.6	4.4
^{240}Pu	2.92	6569	α	5168.3	73.5
			L X-ray	13.6	11.0
^{241}Pu	0.123	14.4	β	5.23(ave)	99.9975
^{242}Pu	0.029	37,580	α	4900.6	78
			L X-ray	13.6	9.1
^{241}Am	trace	432.2	α	5485.74	85.2
			L X-ray	13.9	43
			γ	59.5370	35.9

(a) Information taken from Kocher (1981).

Upon receipt of the foils, the particles were resuspended in 0.06 N NH_4OH using sonication. Separate foils bearing one of three particle sizes (0.66, 1.72, and 3.07 μm d_a) were individually placed in 22 ml glass liquid scintillation vials containing approximately 20 ml of 0.06 N NH_4OH. The vials were tightly capped and partially submerged in the water bath of a sonic cleaner (Bransonic Model 12) for approximately one minute with the cleaner on full power to resuspend the particles.

The stock particle suspensions were then assayed for total alpha activity using a modification of the method of Keough and Powers (1970). The foils were first removed from each of the suspensions and discarded. A small magnetic stir bar was placed in each vial and the suspension was stirred vigorously. While the suspension was stirring, three replicate 100 μl aliquots were placed in 100 ml glass beakers and digested in 8 N nitric acid containing 0.5 N hydrofluoric acid and evaporated to near dryness. The remaining salts were dissolved in 30 ml of 2 N nitric acid containing 2.6% boric acid. Three 0.25 ml aliquots of the nitric-boric acid solution were transferred to 20 ml glass liquid scintillation counting vials containing 15 ml of extractant scintillator solution made by dissolving 200 ml of di(2-ethylhexyl) phosphoric acid in 800 ml of toluene containing 5 grams of terphenyl and 0.05 grams of 1-4-bis-2 (5 phenyloxazolyl) - benzene (POPOP). The vials were capped and counted in a Beckman Model LS-2000 Liquid Scintillation Counter for a sufficient period of time to give $2\sigma \leq 5\%$. The counting efficiency for this system was approximately 100%.

The results from replicates were pooled and the activity concentration of the stock suspension calculated. Table 2 gives the calculated activity concentrations of the stock suspensions.

TABLE 2. Activity Concentrations of Stock Particle Suspensions

d_a (μm)	Activity Concentration (μCi/ml ± S.D.)
3.07	4.593 ± 0.077
1.72	2.437 ± 0.069
0.66	0.3913 ± 0.026

Suspensions for aerosolization were prepared by diluting an aliquot of the stock suspension in sufficient distilled water adjusted to pH 10.0 with concentrated NH_4OH to bring the activity of the final suspension to the desired concentration. Table 3 shows the aerodynamic diameter, physical diameter, and corresponding maximum concentration for 95% single particle production (Raabe 1968) during aerosol generation. The actual concentration used was approximately 85 nCi/ml.

A compressed air operated Lovelace Aerosol Nebulizer was used to generate the test aerosols. A schematic diagram of the experimental apparatus is shown in Figure 1. The actual apparatus, less the aerosol nebulizer, is shown assembled in Figure 2, and disassembled in Figure 3. The test aerosol was generated into a

TABLE 3. Sizes and Limiting Concentrations of Particle Suspensions

d_a (μm)	Physical Diameter (μm)	Maximum Concentrations For 95% Singlet Production Particles/ml	μCi/ml
0.66	0.14	3.5×10^8	0.25
1.72	0.48	3.5×10^8	10.0
3.07	0.93	3.5×10^8	73.0

section of 1.27 cm I.D. copper tubing 48 cm long. A small flow (10 l/m) of dry dilution air was injected into the aerosol stream just downstream of the aerosol generator to facilitate drying of the aerosol. The copper tubing was heated via electrical resistance heat tape to approximately 150°C to further dry the aerosol. The dried aerosol was then injected into a venturi-like apparatus and mixed with clean (HEPA-filtered) dilution air at 20°C and 30% relative humidity before being collected on a glass-fiber filter held in a Gelman Model 2220 stainless steel filter holder. A new aerosol generator was used for each test aerosol to avoid cross-contamination. The system was flushed with clean dilution air at 150 lpm between aerosols to remove loosely attached particles and avoid re-entrainment of particles during experiments.

A dry-test meter was used to calibrate a differential pressure gauge which measured the pressure-drop across a constriction in the vacuum line. Sampling velocity was calculated as the quotient of the flow rate in m^3/sec and the cross-sectional area of the filter

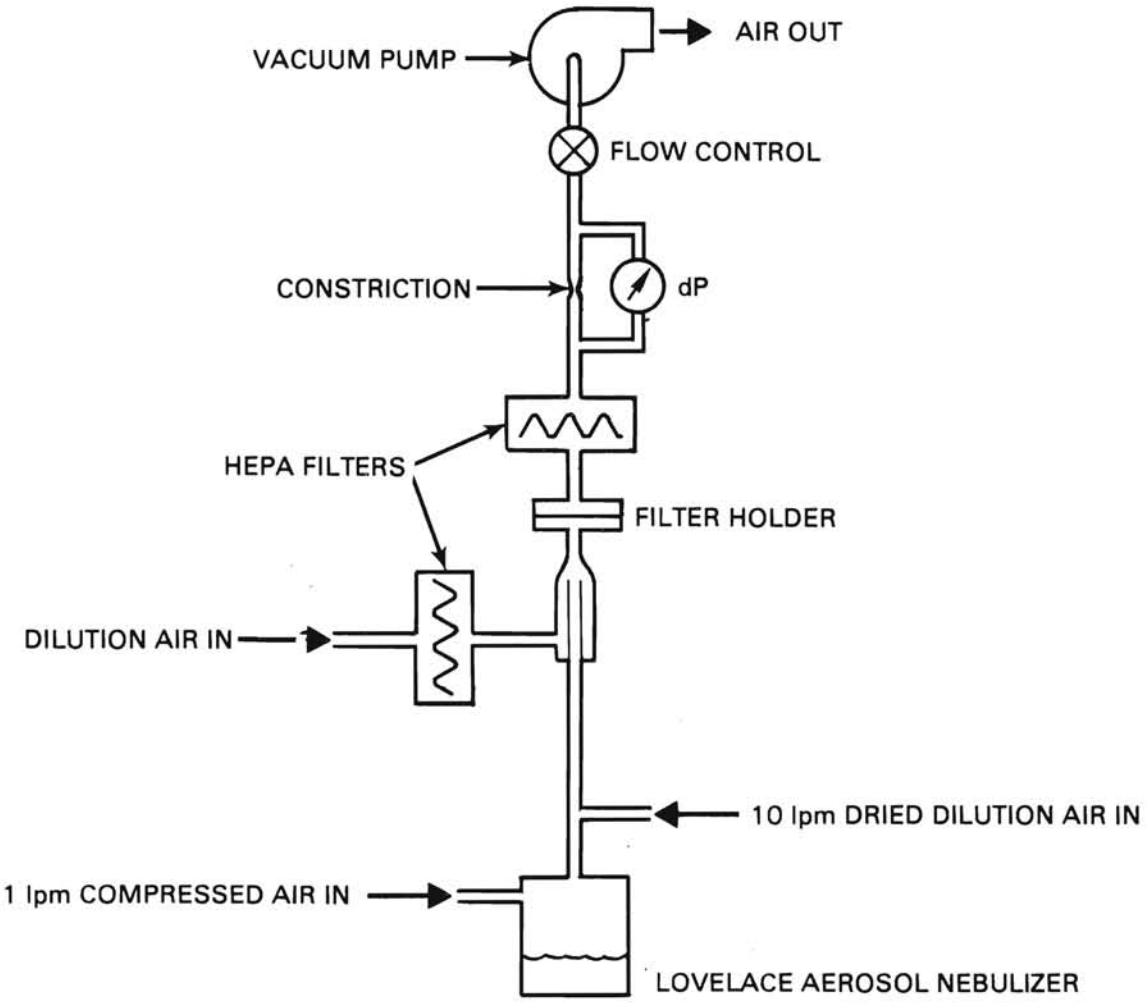

FIGURE 1. Schematic Diagram of Aerosol Generation and Sampling Apparatus

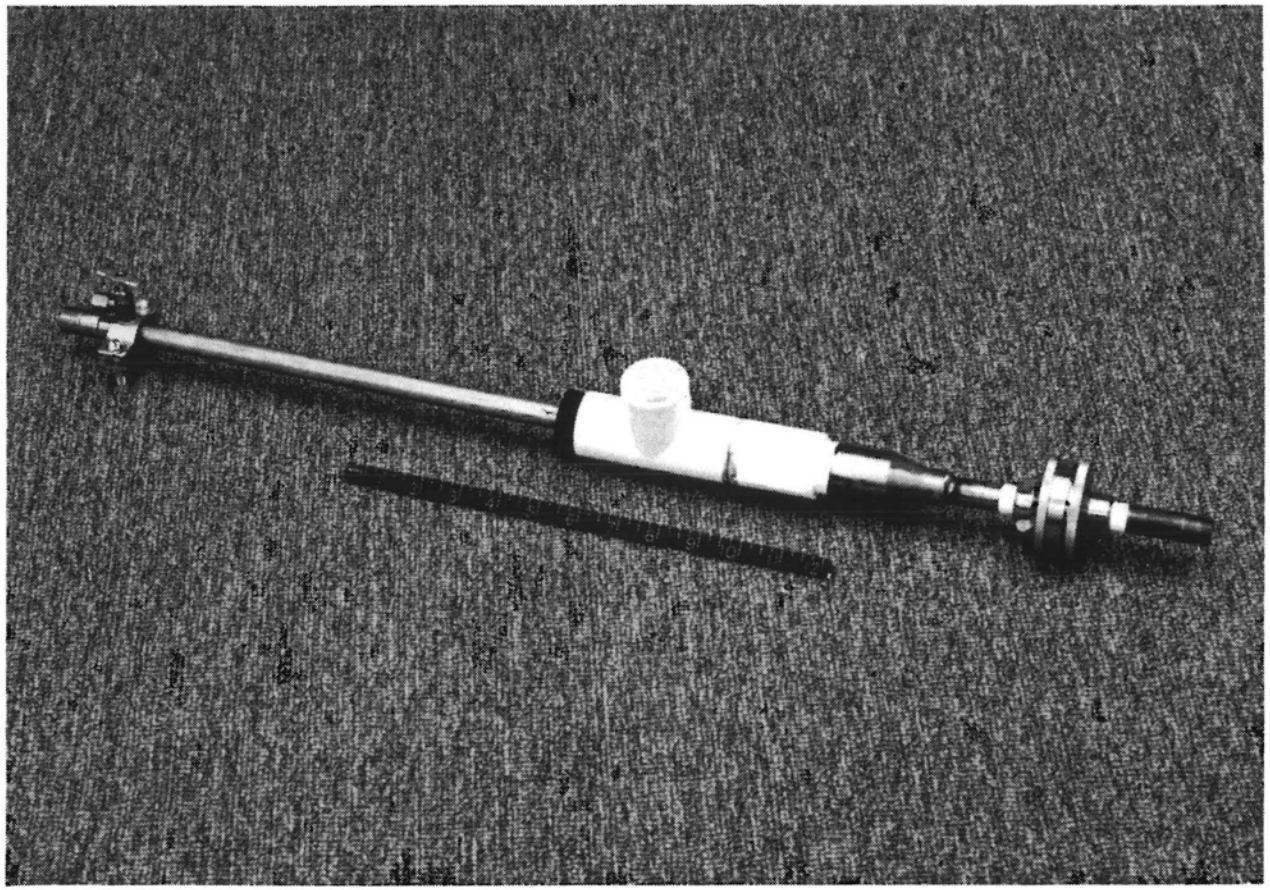

FIGURE 2. Aerosol Sampling Apparatus, Assembled

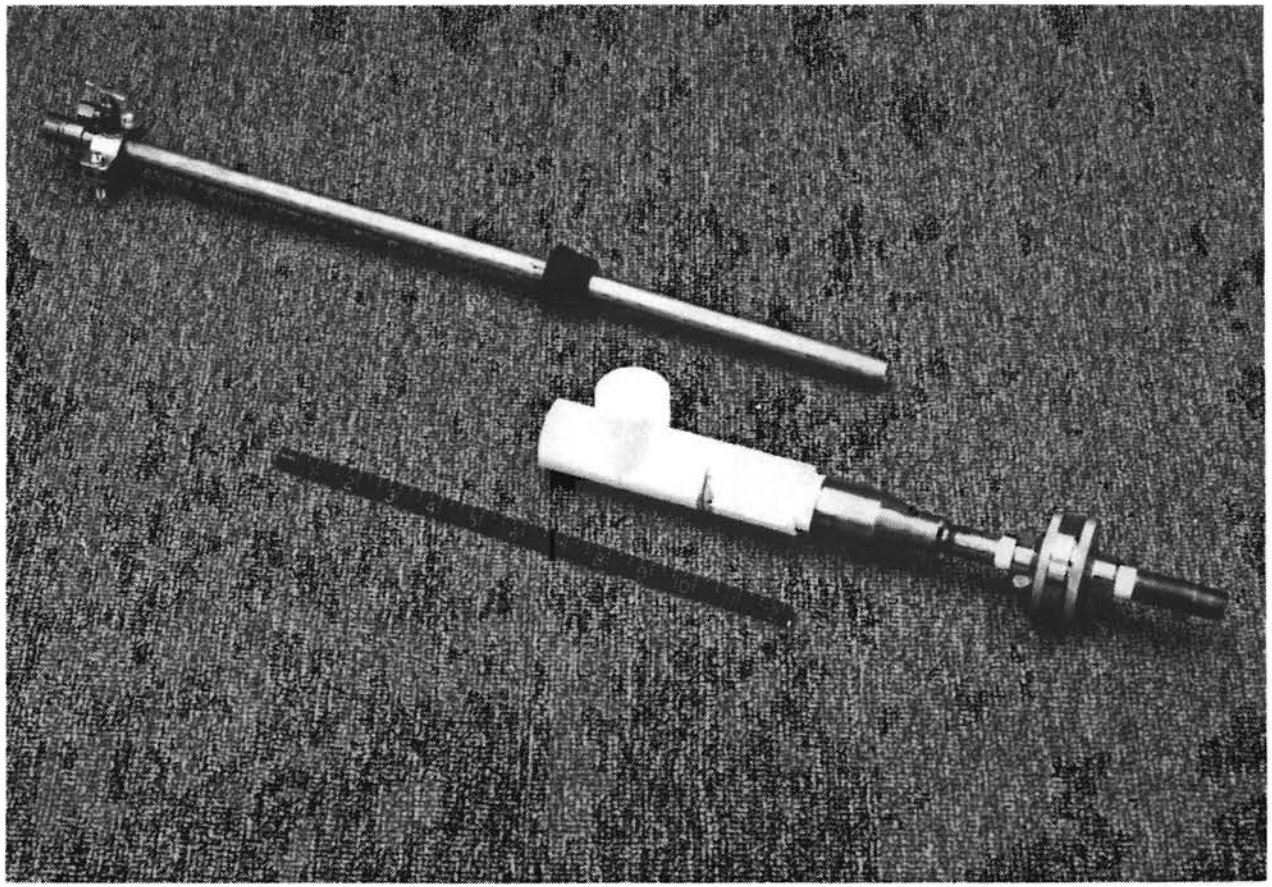

FIGURE 3. Aerosol Sampling Apparatus, Disassembled

in m^2. The sampling velocity was controlled by a valve in the vacuum line downstream from the pressure gauge.

Three replicate samples of each aerosol were collected at each of four sampling velocities. Table 4 shows the velocities in the mixing chamber, flow rates, and corresponding Reynolds numbers used in the experiments. The flow rates and velocities used correspond to the range of sampling flow rates commonly used in occupational air sampling. Sampling times were ajusted so that 113 liters of air were drawn through each sample.

TABLE 4. Flow Rates, Velocities, and Corresponding Reynolds Numbers

Flow Rate (lpm)	Velocity (m/sec)	Re
28	7	5,900
57	14	12,000
85	21	18,000
113	28	23,000

The Reynolds Number (Re) is a dimensionless quantity that characterizes fluid-flow through a pipe or around an obstacle. Re is given by

$$Re = \frac{\rho V d}{\eta}$$

where ρ is the density of the fluid, V is the relative velocity between the fluid and the wall of the pipe, d is the inside diameter of the pipe, and η is the coefficient of viscosity. Flow through

pipes is turbulent for Re > 4,000. Turbulent flow ensures good mixing of aerosol and dilution air (Hines 1982).

In addition to the glass-fiber filter samples, a sample of each test aerosol was collected on 1.0 μm nuclepore filters for analysis by scanning electron microscopy.

The filters used in this study were Hollingsworth and Vose Model LB-5211 47 mm glass-fiber filters. The downstream side of these filters is laminated with a fibrous polyester backing material to provide physical strength and the base material consists of micro-glass fibers with an average fiber diameter of 0.4 - 0.7 μm. Table 5 gives the manufacturer's specifications for LB-5211 paper.

TABLE 5. Manufacturers Specifications for LB-5211 Filter Paper

Average Fiber Diameter (μm)	0.4 - 0.7
Thickness (cm)	0.04
DOP Smoke Penetration at 32 l/m (%)	0.016
Air Flow Resistance (mm of water) at 32 l/m	38.

Exposed filters were analyzed for total ^{241}Am and plutonium as ^{239}Pu using photon spectrometry. The signal from a Princeton Gamma Tech Model IGP2013 intrinsic germanium detector was analyzed using a Nuclear Data Model 66 8,000 channel analyzer. Photopeaks were quantified by first transforming the number of counts per channel (x) using the transformation $\sqrt{x} + \sqrt{x+1}$ to stabilize variance (Anscombe 1948, Freeman and Tukey 1950). Assuming that the counts

are Poisson distributed, this transformation yields a variable with variance and standard deviation equal to 1. Transformed data were then smoothed using an asymetric 7-point moving median. Intrinsic germanium photopeaks from plutonium consisted of 3 channels or less. This smoothing procedure tends to annihilate peaks of 7 consecutive points or less and provides an estimate of the background counts in each photopeak (Velleman 1980). The smoothed data were then subtracted from the transformed data channel by channel. Any difference greater than 2 indicated with 95% confidence that the counts in that channel were significant. Data from channels with significant counts were then back-transformed, the background subtracted, channels in each photopeak summed and the count rate in each photopeak due to plutonium calculated. The 13.6 keV x-ray of ^{239}Pu was used to quantify ^{239}Pu and to minimize ^{241}Am interference. Attenuation of this energy photon in the fibers was insignificant. The 59.54 keV gamma-ray of ^{241}Am was used to quantify ^{241}Am. These two radionuclides accounted for over 99% of the radioactivity detected. The photon-spectrometry apparatus was calibrated against National Bureau of Standards (NBS)-traceable standards. The distribution of activity on the standards matched that of the samples.

Direct alpha counts of each filter were made using an Ortec Model R-450-100 450 mm^2 ruggedized surface barrier detector. The signal from the detector was amplified and passed through a single channel analyzer to a scaler. Gross counts were recorded on a Silent 700 Printer. Counts were made in air, with a fixed source to

detector distance of 5 mm. The equipment was calibrated using an NBS-traceable plated ^{239}Pu standard whose activity distribution matched that of the filters.

The distribution of activity on filters exposed to plutonium aerosols in the sampling apparatus was determined in the following manner. A series of annular shields with an outer diameter of 47 mm and a varying inner diameter were cut from heavy construction paper. These shields were laid one after the other, starting with the largest inner diameter, on top of exposed filters and the filters were counted by direct alpha counting. The resulting counts were plotted as percent of maximum activity detected versus inner diameter of the annulus. The smallest diameter at which the maximum activity was obtained indicated the maximum distribution of activity on the filter.

Alpha spectrometry of filter samples was performed using a separate Ortec Model R-450-100 ruggedized surface barrier detector. The signal from the detector was amplified and routed to a Davidson Model 1056 multi-channel analyzer. Filters were placed in an evacuated vacuum chamber with a fixed source to detector distance of 1 cm. Data from the multi-channel analyzer were recorded on magnetic tape and transferred to a Hewlett-Packard 1000E mini-computer for processing, using commercially available graphics software. The spectra obtained from filter samples were compared with spectra obtained from aliquots of the stock particle suspensions evaporated on glass coverslips.

Samples were prepared for autoradiography by embedding the filters in glycol methacrylate followed by thin sectioning and mounting on glass slides. Duplicate slides were dipped in Ilford Nuclear K-5 Gel Emulsion and exposed for varying periods up to 12 weeks prior to developing and examination by light microscopy. Particles deposited on glass slides or nuclepore filters were prepared for scanning electron microscopy by sputter coating the specimen with a thin layer of gold, approximately 200 nm thick, and then viewed with a JEOL Model JSM-255III Scanning Electron Microscope.

The ranges of plutonium and americium alpha particles in glass were calculated according to Mayneord and Hill (1969). Range in glass was interpolated from that in water using the Bragg-Kleeman rule, according to which

$$\frac{R_a \rho_a}{R_b \rho_b} = \frac{A_a^{\frac{1}{2}}}{A_b^{\frac{1}{2}}}$$

where R is the range of alpha particles in the medium in centimeters; ρ is the density of the medium in grams per cubic centimeter; and $A^{\frac{1}{2}}$ is the square root of the effective atomic weight of the medium. $A^{\frac{1}{2}}$ is given by

$$A^{\frac{1}{2}} = \frac{N_1 A_1 + N_2 A_2 + N_3 A_3 \ldots}{N_1 A_1^{\frac{1}{2}} + N_2 A_2^{\frac{1}{2}} + N_3 A_3^{\frac{1}{2}} \ldots}$$

where N_1, N_2, N_3 . . . are the known atom fractions in the medium. The range of alpha particles in water was derived from the range of

protons in water based on the assumption that an alpha particle of energy 3.97E has a range equal to 0.993 times the range of a proton of energy E. Proton ranges in water were obtained from Bichsel (1968). The atom fractions in glass were calculated from the elemental composition of LB-5211 filter fibers provided by the manufacturer (Masters 1983) and shown in Table 6.

TABLE 6. Composition of LB-5211 Glass Fiber

Compound	% by Weight
SiO_2	57.9
B_2O_3	10.7
Na_2O	10.1
Al_2O_3	5.8
Fe_2O_3	0.1
BaO_2	5.0
ZnO	3.9
K_2O_2	2.9
CaO-MgO	3.0
F_2O	0.6
	100.0

The atom fraction is given by:

$$F_i = \frac{n_i}{\sum_i n_i}$$

where n_i is the number of atoms per gram of element "i". n_i is given by

$$n_i = \left(\frac{N \quad A_i}{W_i} \right)$$

where W_i is the weight percent of element "i", A_i is the atomic weight of element "i", and N is Avogadro's Number.

For evaluation of counting losses due to burial in the filter matrix, the fraction detected by direct alpha count was calculated as the ratio of activity detected by direct alpha count to the quantity determined by photon spectrometry. The fraction detected (f) was tested for significance using a one tailed t-test at the 95% confidence level against the null hypothesis: f=1, where f=1 indicated no burial losses.

RESULTS AND DISCUSSION

Figure 4 shows the relationship between velocity at the filter face and pressure drop as measured across a constriction in the sampling apparatus. Velocity was calculated from flow measurements based on the known diameter of the flow-path at the filter face.

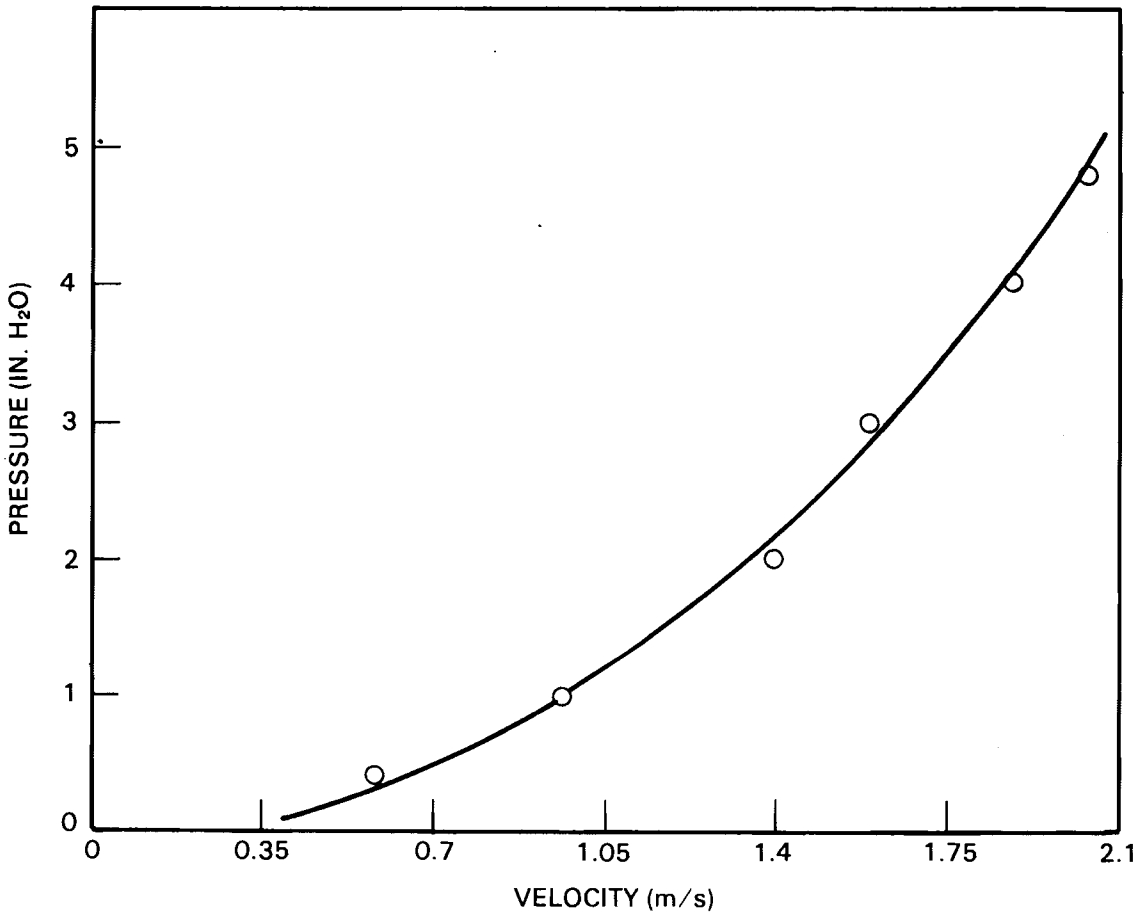

FIGURE 4. Sampling Velocity vs Pressure Drop Calibration Curve

Figure 5 summarizes the data obtained from activity distribution measurements of filters exposed to plutonium aerosols in the sampling apparatus. From these data, it was determined that the activity on the filters was distributed in a circular area approximately 37 mm in diameter centered in the middle of the filter. NBS-traceable ^{239}Pu calibration sources with identical activity distribution were used to calibrate all counting equipment used in this study.

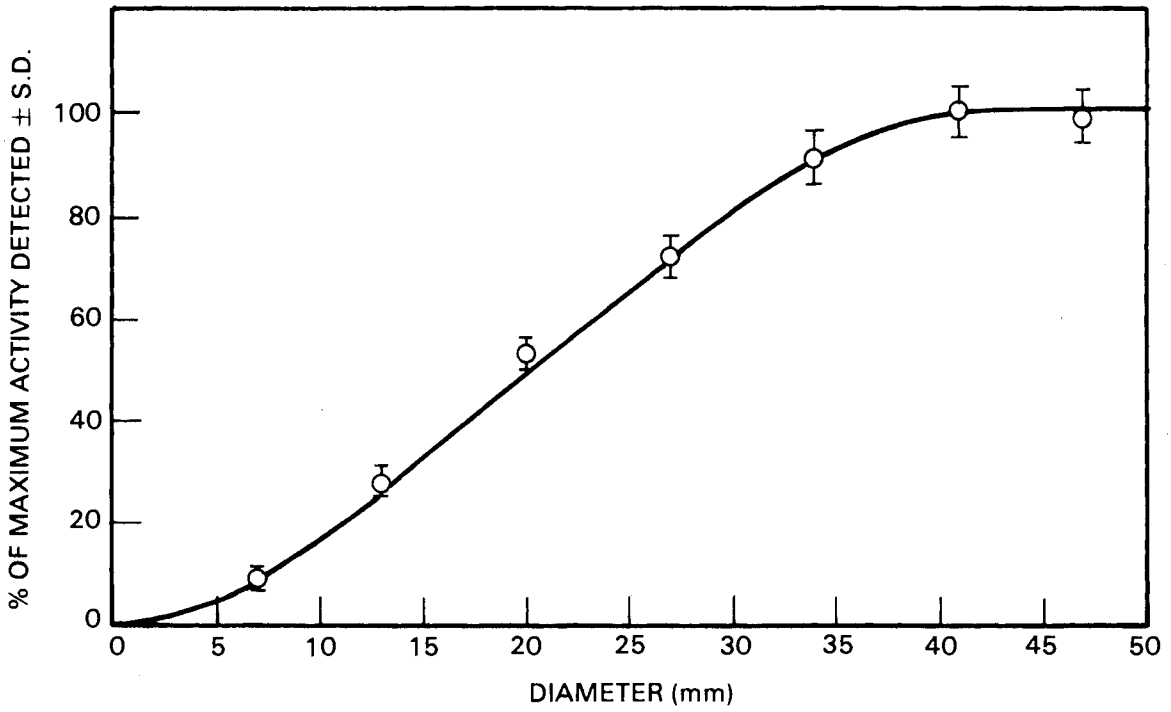

FIGURE 5. Activity Distribution of Filters Exposed to Plutonium Aerosols

Atom fractions of elements in LB-5211 glass fibers are shown in Table 7. Based on these fractions, the effective atomic weight of LB-5211 glass was calculated as 21.5 gram/mole. The calculated ranges of plutonium and americium alpha particles in water and glass are shown in Table 8.

Figures 6 - 8 are scanning electron micrographs showing evaporated aliquots of the particle suspensions. The disparity in numbers of particles per frame is due to different magnifications and to the fact that the suspensions were adjusted to the same activity concentration, but different number concentrations. The figures illustrate the relatively monodisperse character of the

TABLE 7. Atom Fraction of Elements in LB-5211 Glass Fibers

Element	A	Weight % in Glass	Atom Fraction
O	16	47.3	0.609
Si	28	27.0	0.198
Na	23	7.5	0.068
B	11	3.4	0.058
Al	27	3.1	0.024
Zn	65	3.1	0.010
K	39	2.1	0.011
Ca	40	2.1	0.011
Ba	137	4.1	0.006
F	19	0.4	0.004
Fe	56	trace	---

TABLE 8. Ranges of Plutonium and Americium Alpha Particles in Water and Glass

Isotope	Energy (keV)	Intensity %	Range (gm/cm^2) Water	Glass
^{238}Pu	5499.21	71.6	0.0055	0.0040
^{239}Pu	5155.4	73.3	0.0050	0.0037
^{240}Pu	5168.3	73.5	0.0052	0.0037
^{242}Pu	4900.6	78.0	0.0047	0.0035
^{241}Am	5485.74	85.2	0.0054	0.0038

particle suspensions, although it can be seen that the distribution of particle sizes is wider in the 0.66 μm suspension than in the 1.72 and 3.07 μm suspensions because of poorer resolution capability of the LAPS for smaller particle sizes. Table 9 shows the physical size distribution of the particles in the evaporated suspensions (shown in Figures 6 - 8) obtained with a Tracor-Northern TN-2000 analyzer equipped with a commercially available particle recognition and characterization code. These data are in good agreement with the physical diameters shown in Table 3.

TABLE 9. Physical Diameters of Particles in Evaporated Suspensions

Nominal Aerodynamic Diameter, μm d_a	Average Physical Diameter, μm ± S.D.
0.66	0.25 ± 0.34
1.72	0.58 ± 0.12
3.07	1.02 ± 0.34

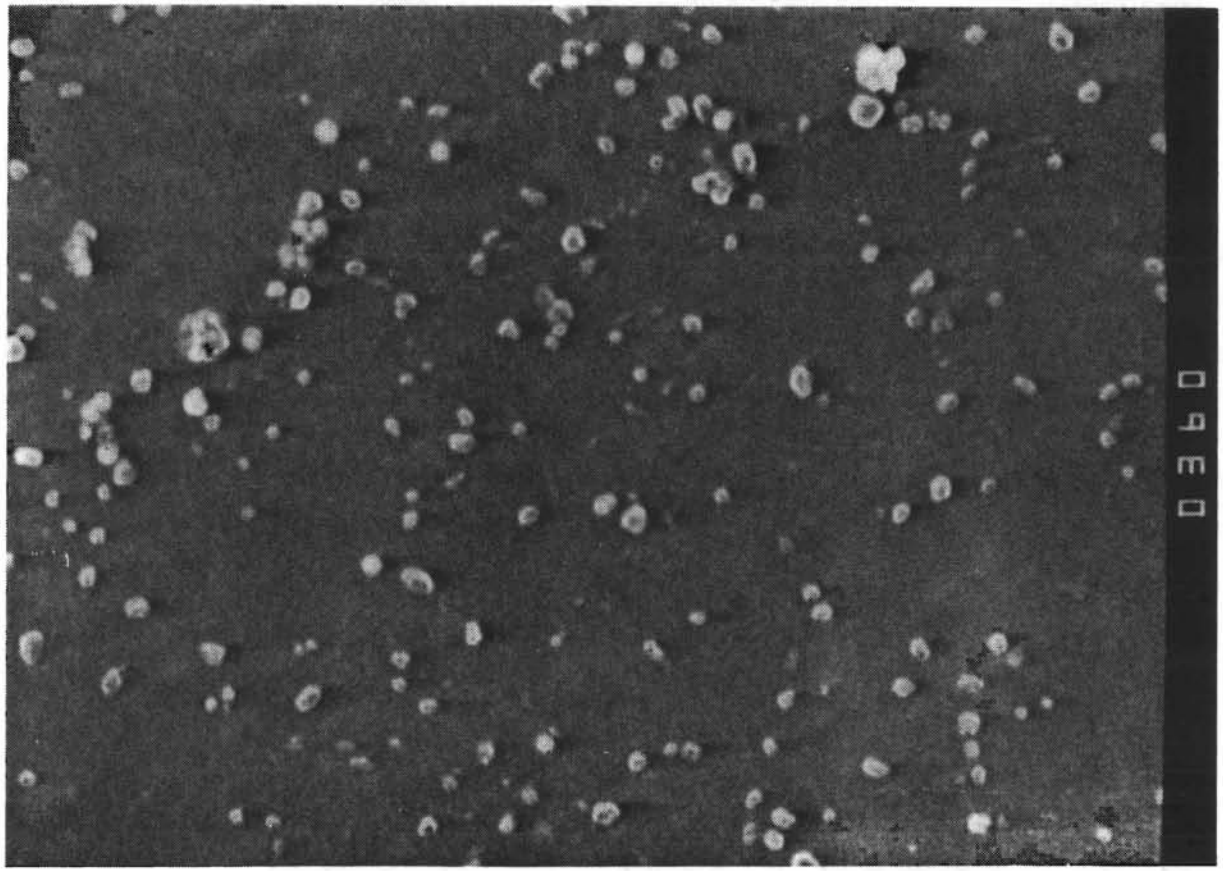

FIGURE 6. Evaporated 0.66 μm (d_a) Particle Suspension, 17,500x.

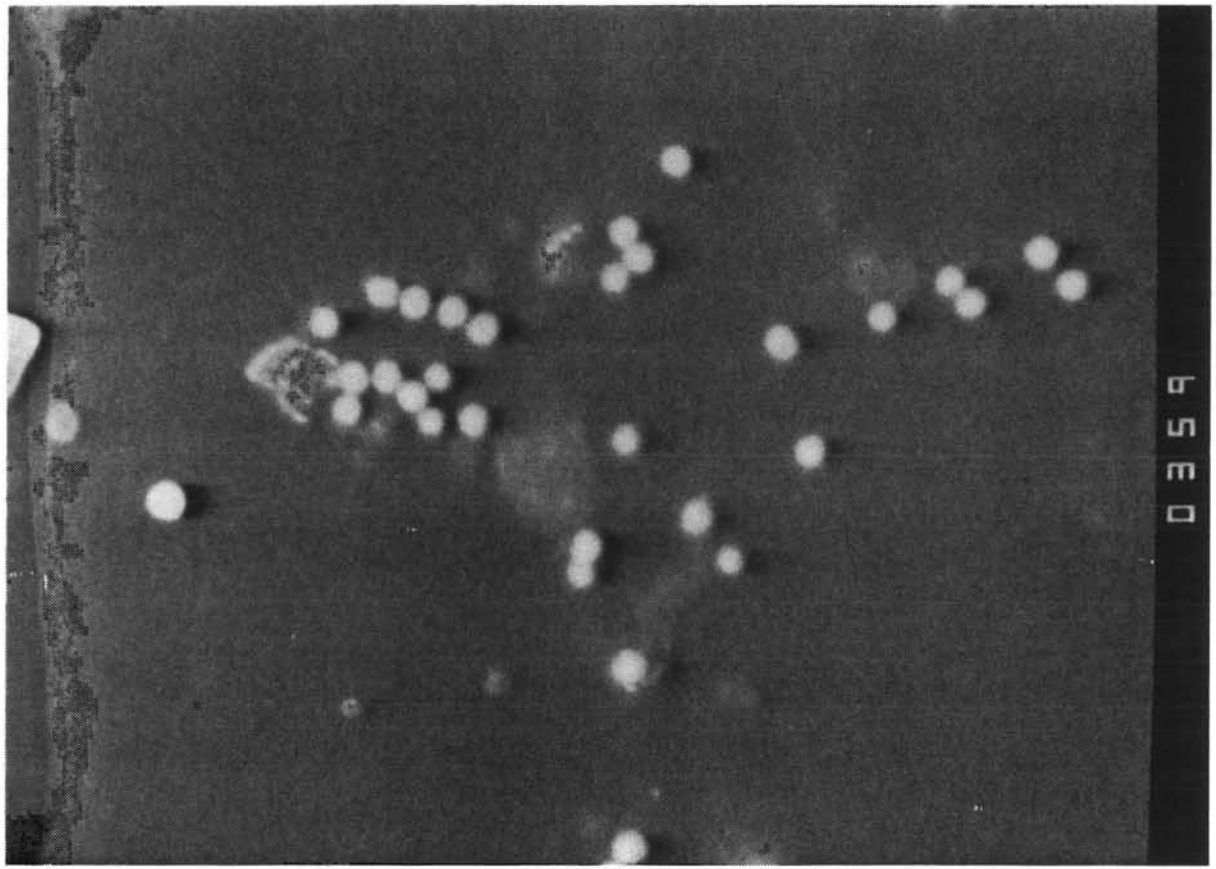

FIGURE 7. Evaporated 1.72 μm (d_a) Particle Suspension, 12,250x.

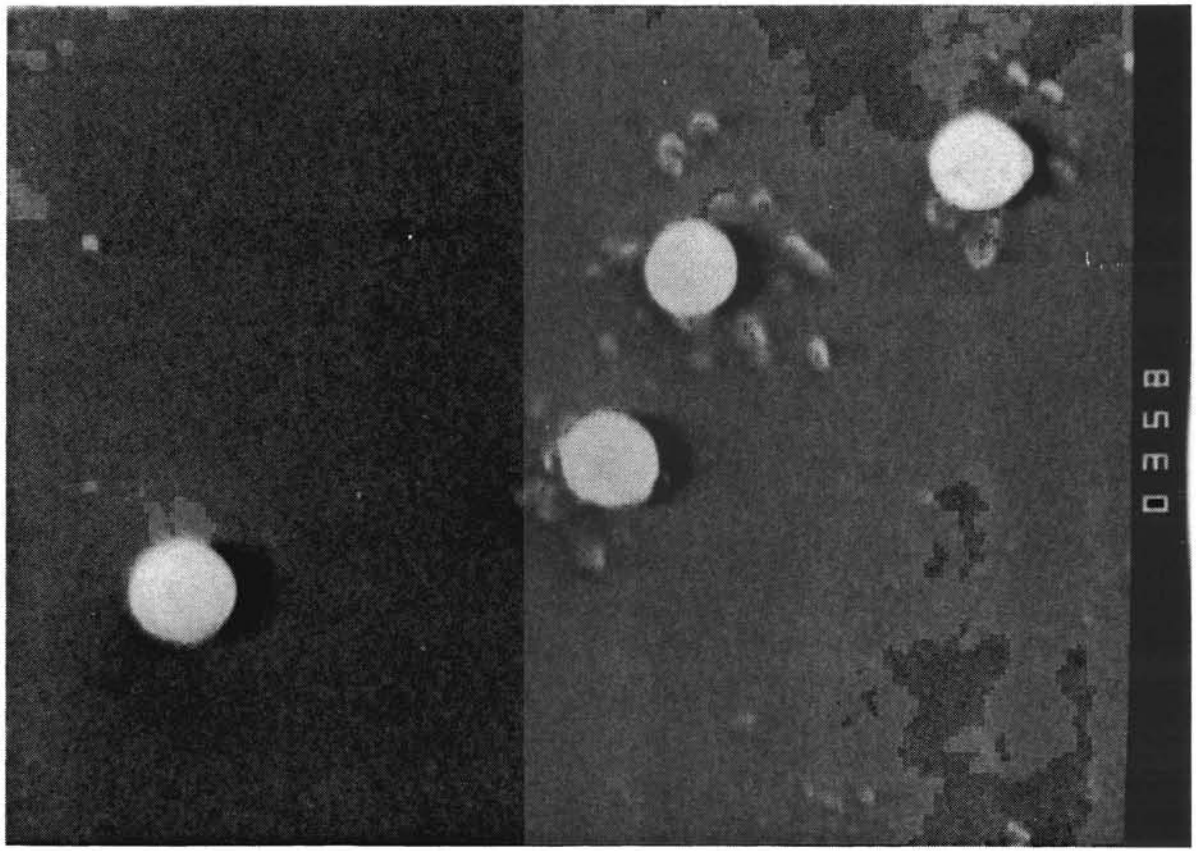

FIGURE 8. Evaporated 3.07 μm (d_a) Particle Suspension, 17,500x.

Figures 9 - 11 are scanning electron micrographs of the aerosol particles used in the experiment collected on 1 μm pore-size nuclepore filters after being aerosolized. Particles containing plutonium were identified using electron dispersive spectrometry and are circled in the photographs. Particle agglomeration was not observed and the absence of an evaporation ring around each particle indicates that the aerosols were adequately dried. Not all of the particles in these figures are plutonium dioxide. Many of the particles, primarily the ones with irregular, non-spherical shapes, were identified as being high in silicon content. The source of these particles was unknown, but was suspected to be the air drying columns used during aerosol generation.

Alpha energy spectra obtained from filters under varying conditions of particle size and velocity are shown in Figures 12 - 21. Superimposed on each filter spectrum is a reference spectrum obtained from an aliquot of the corresponding particle suspension evaporated on a glass slide. Differences between the filter spectra and the reference spectra can be attributed to scattering and/or absorption within the filter matrix. Increased straggling was observed in several of the filter spectra.

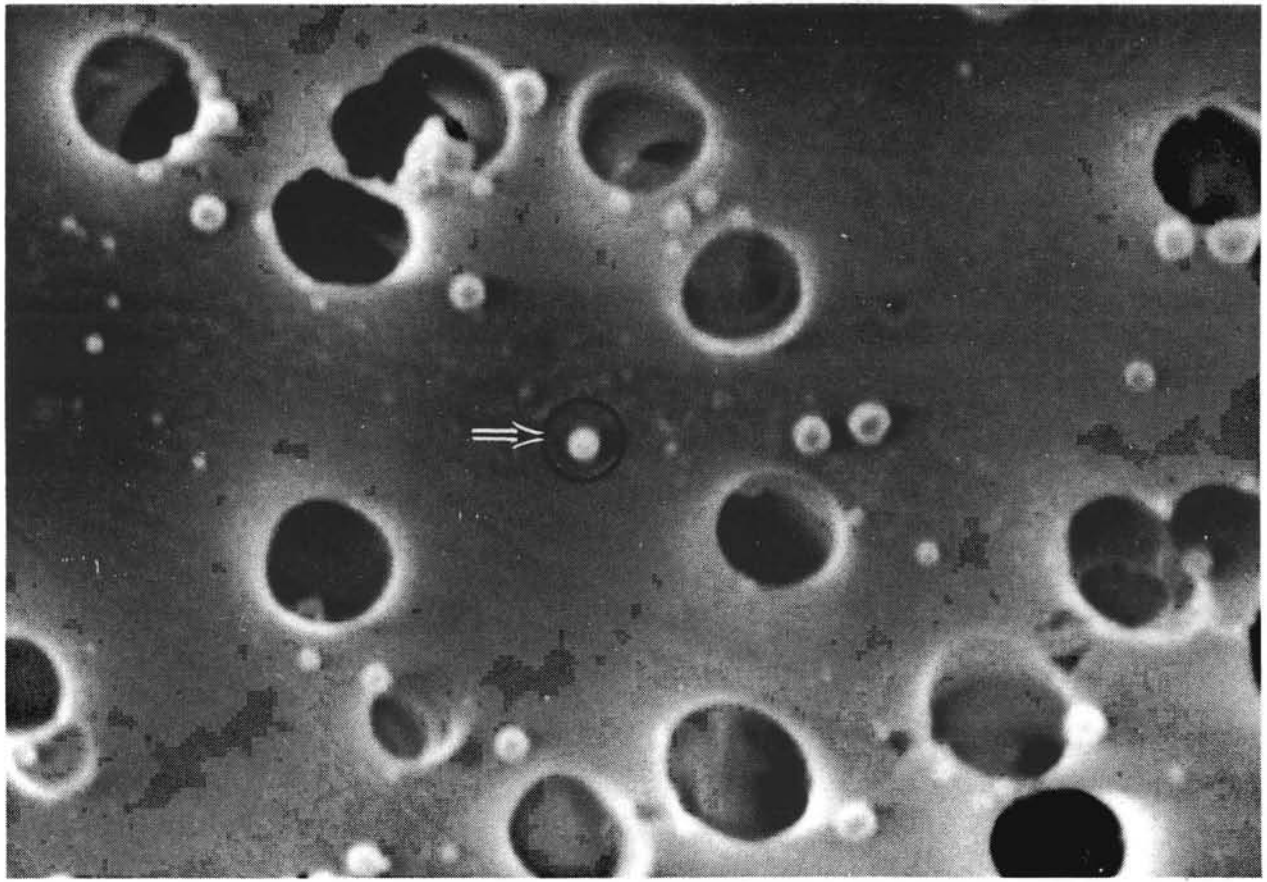

FIGURE 9. 0.66 μm (d_a) Aerosol Collected on 1 μm Nuclepore Filter, 17,500x.

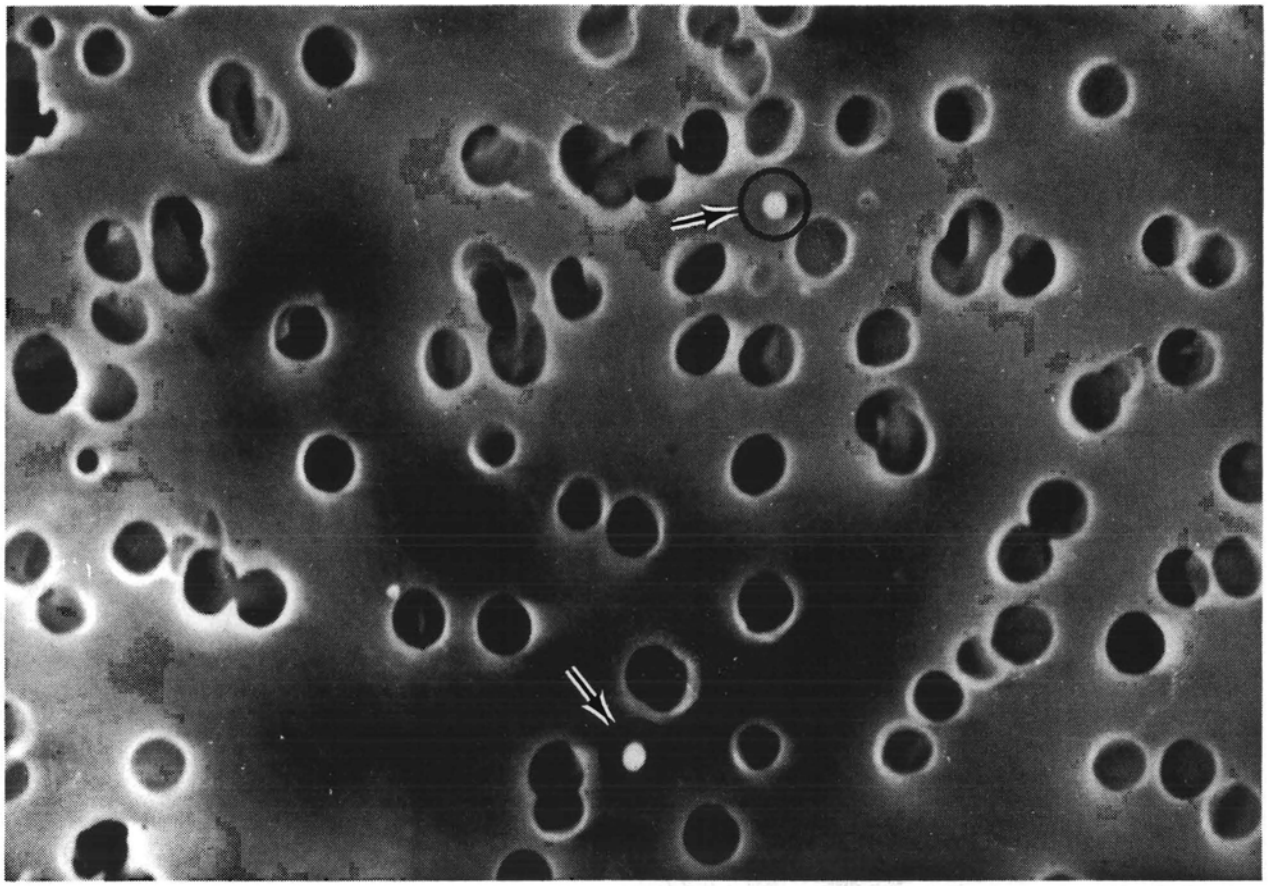

FIGURE 10. 1.72 μm (d_a) Aerosol Collected on 1 μm Nuclepore Filter, 7,800x.

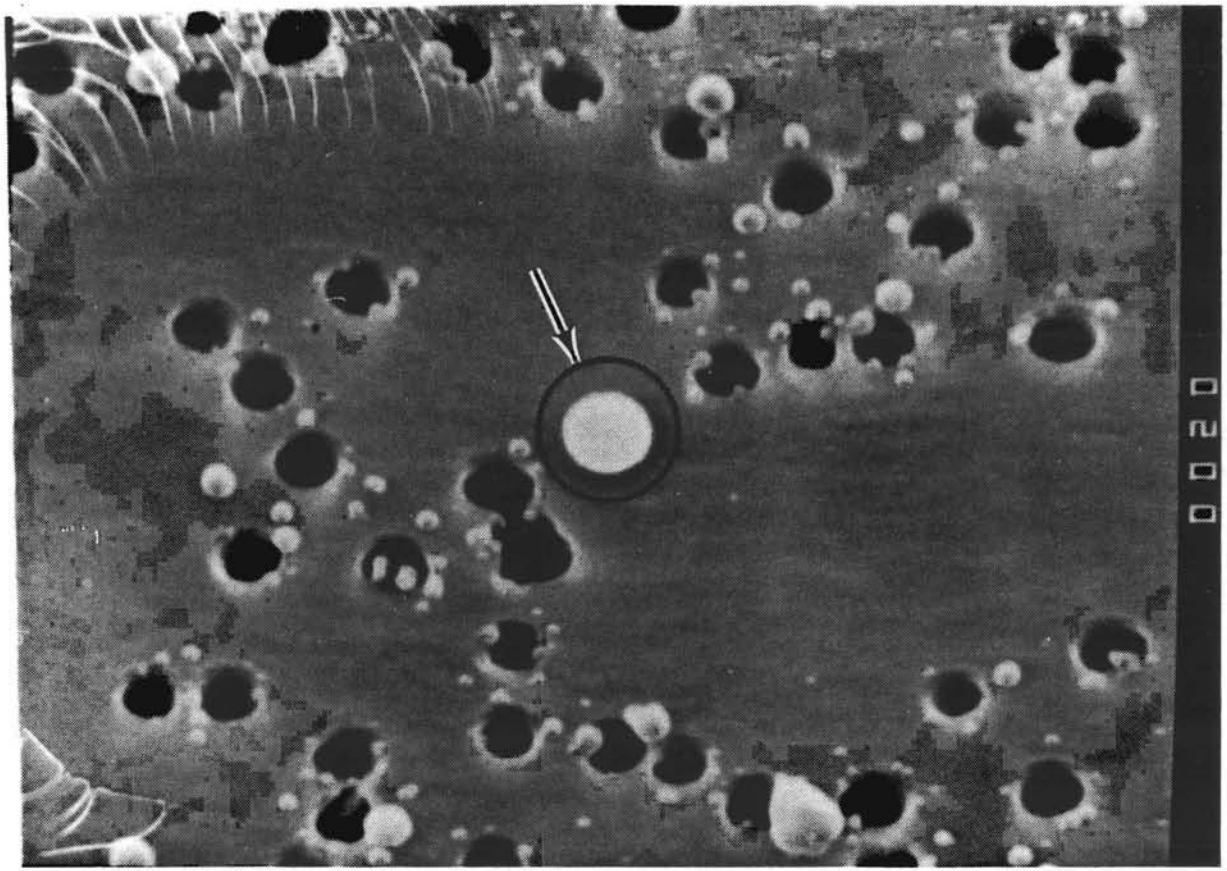

FIGURE 11. 3.07 μm (d_a) Aerosol Collected on 0.6 μm Nuclepore Filter, 17,500x.

Table 10 summarizes the results of alpha energy resolution comparison between filters. Alpha energy resolution was calculated as the full width at half-maximum divided by the peak energy and is expressed as percent of peak energy. Alpha energy resolution is not clearly a function of particle size or sampling velocity, although resolution is somewhat degraded in most cases.

TABLE 10. Alpha Energy Resolution as Percent of Peak Energy for Various Aerodynamic Particle Sizes and Sampling Velocities

	Aerodynamic Diameter (μm)		
	0.66	1.72	3.07
Reference Source Velocity (m/s)	4	4	4
0.5	7	3	5
1	6	4	7
1.5	4	4	6
2	4	8	6

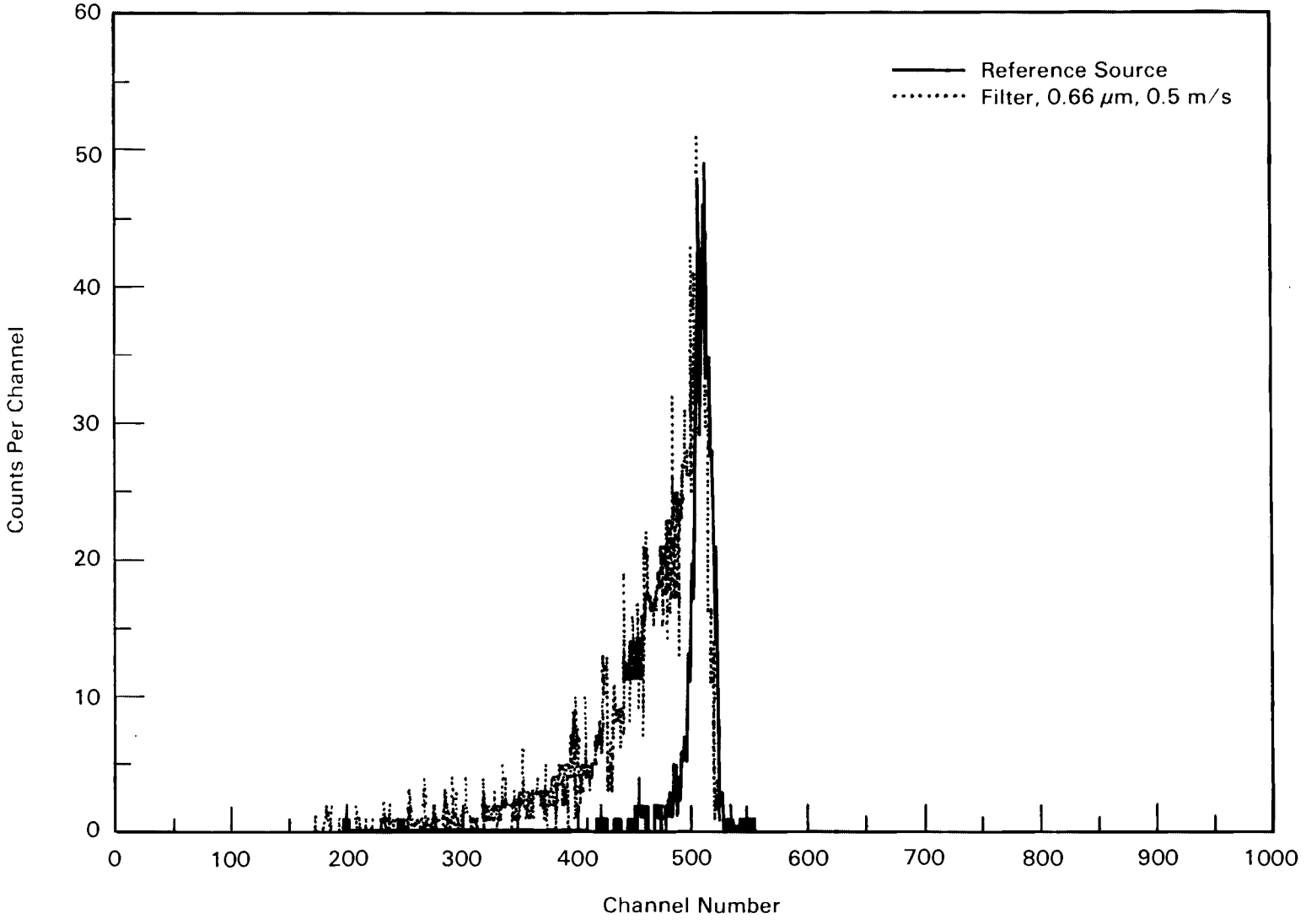

FIGURE 12. Alpha Energy Spectrum of 0.66 μm $^{239}PuO_2$ Deposited on LB-5211 Filter Paper at 0.5 m/s

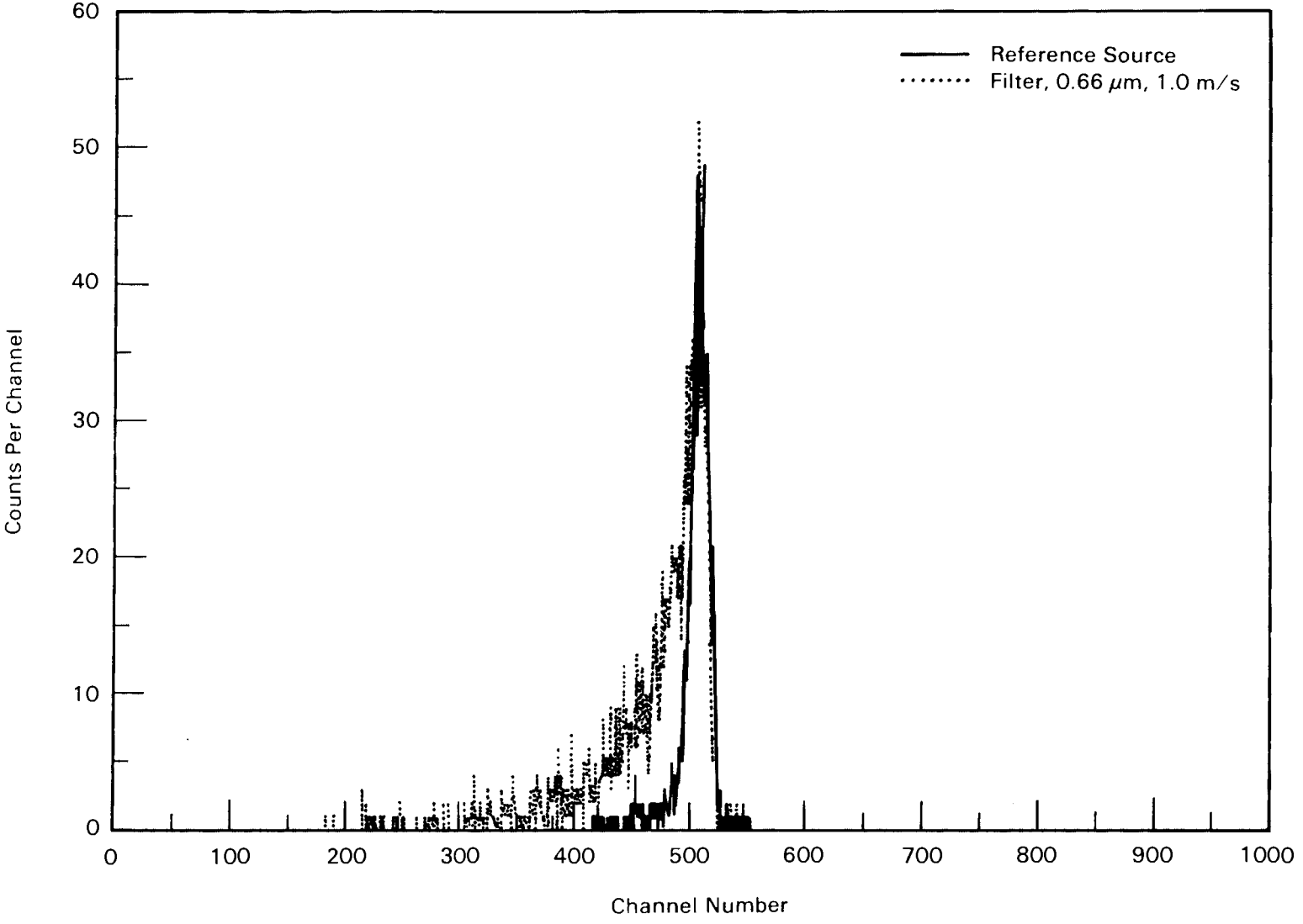

FIGURE 13. Alpha Energy Spectrum of 0.66 μm $^{239}PuO_2$ Deposited on LB-5211 Filter Paper at 1 m/s

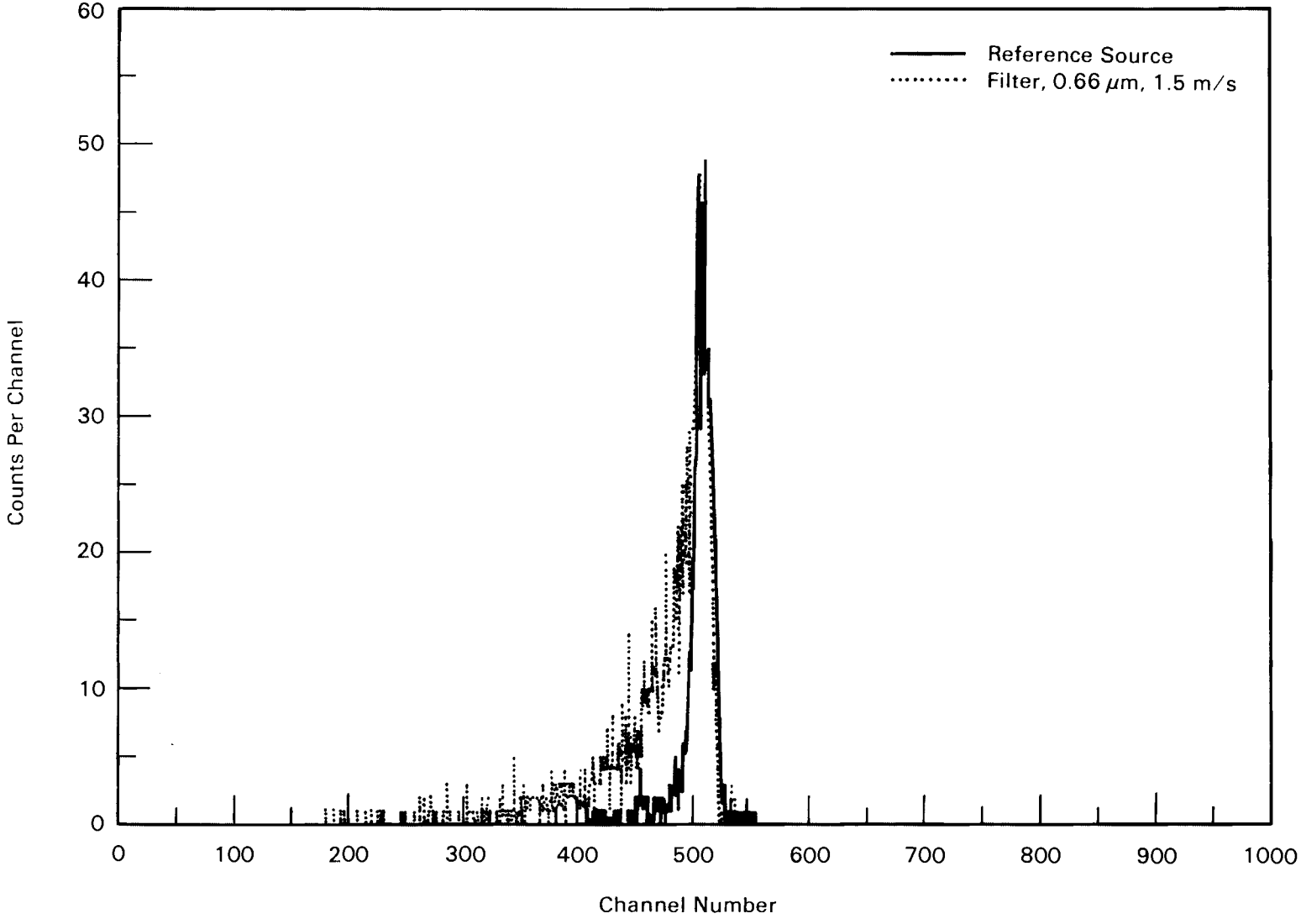

FIGURE 14. Alpha Energy Spectrum of 0.66 μm $^{239}PuO_2$ Deposited on LB-5211 Filter Paper at 1.5 m/s

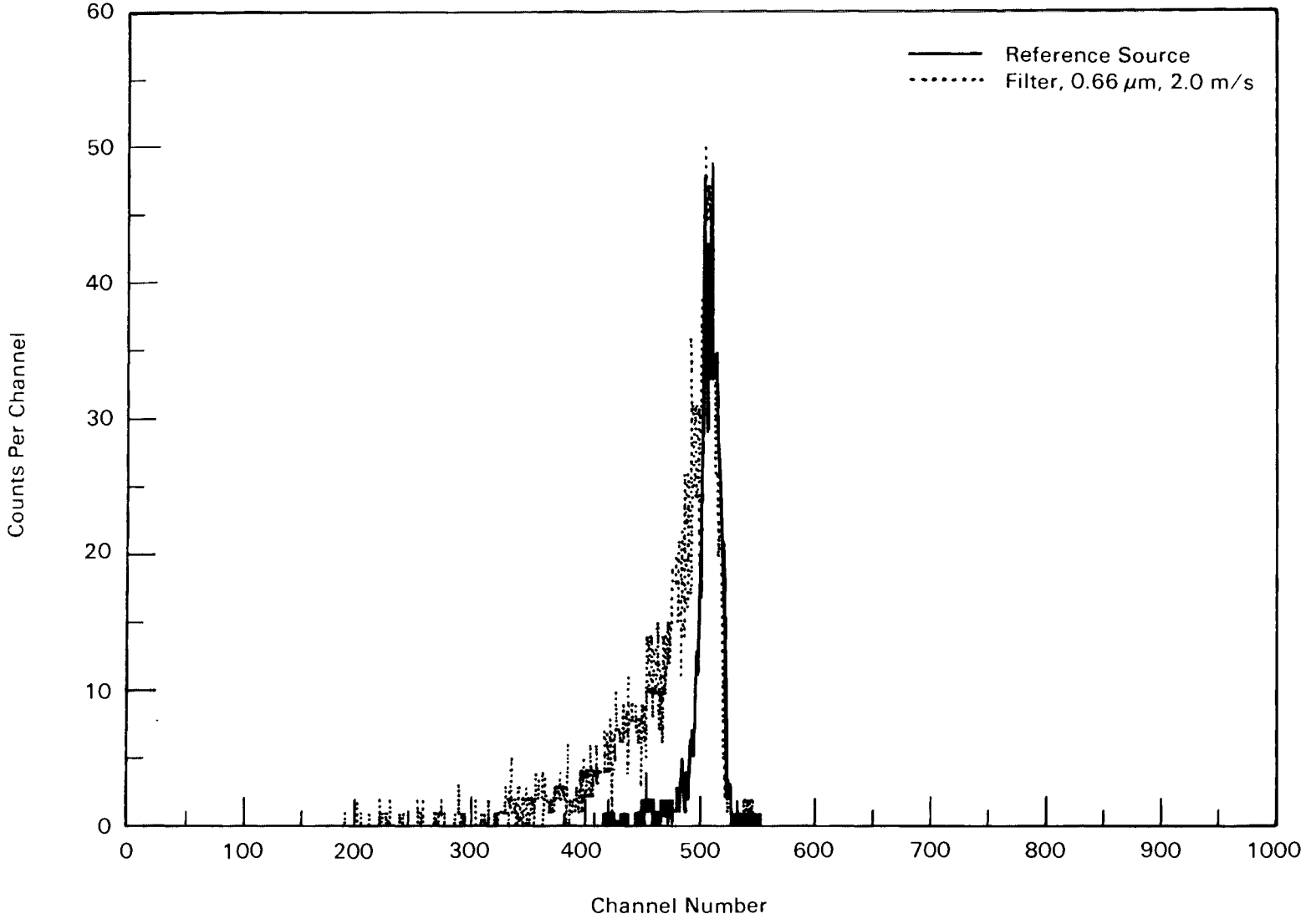

FIGURE 15. Alpha Energy Spectrum of 0.66 μm $^{239}PuO_2$ Deposited on LB-5211 Filter Paper at 2 m/s

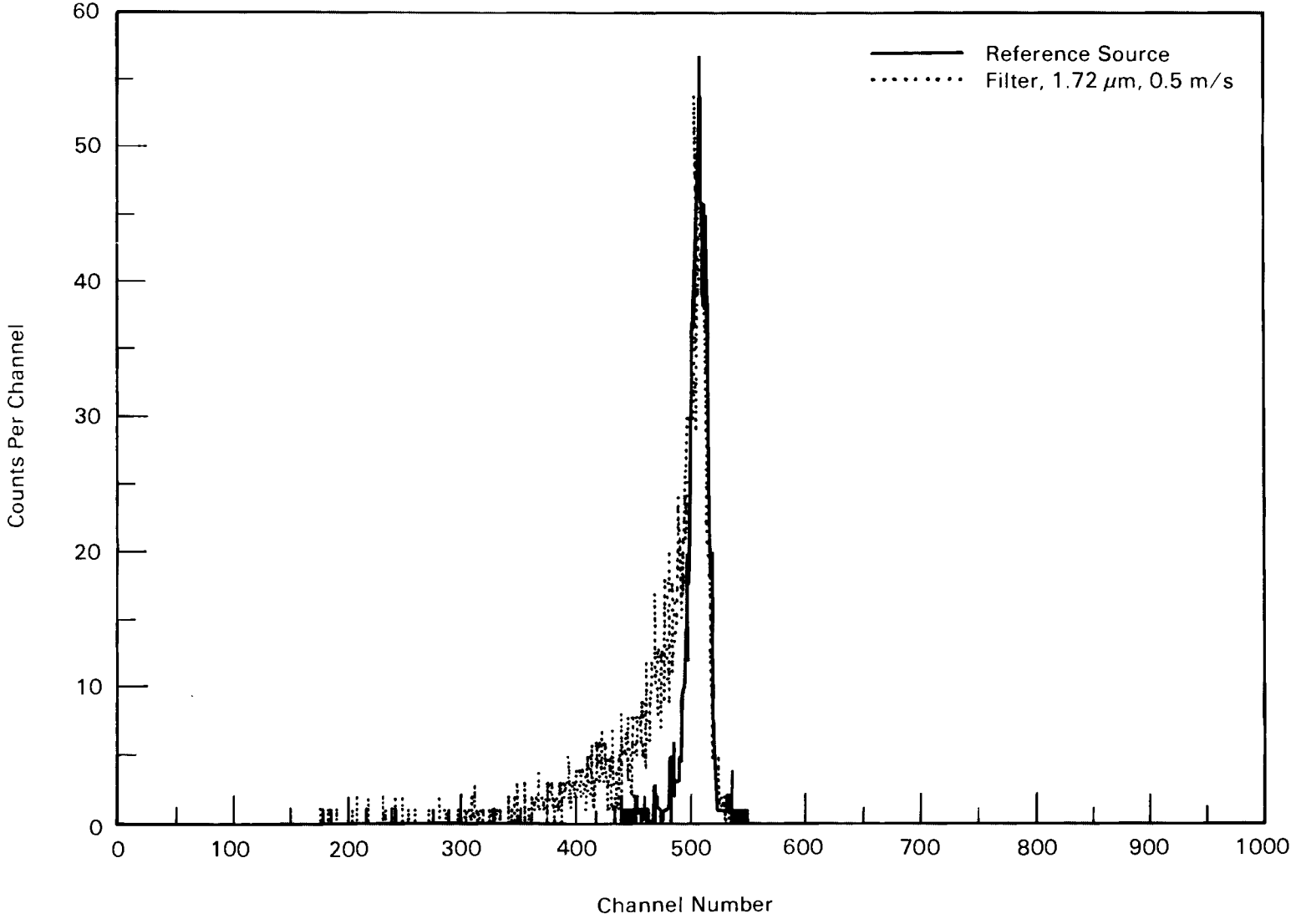

FIGURE 16. Alpha Energy Spectrum of 1.72 μm $^{239}PuO_2$ Deposited on LB-5211 Filter Paper at 0.5 m/s

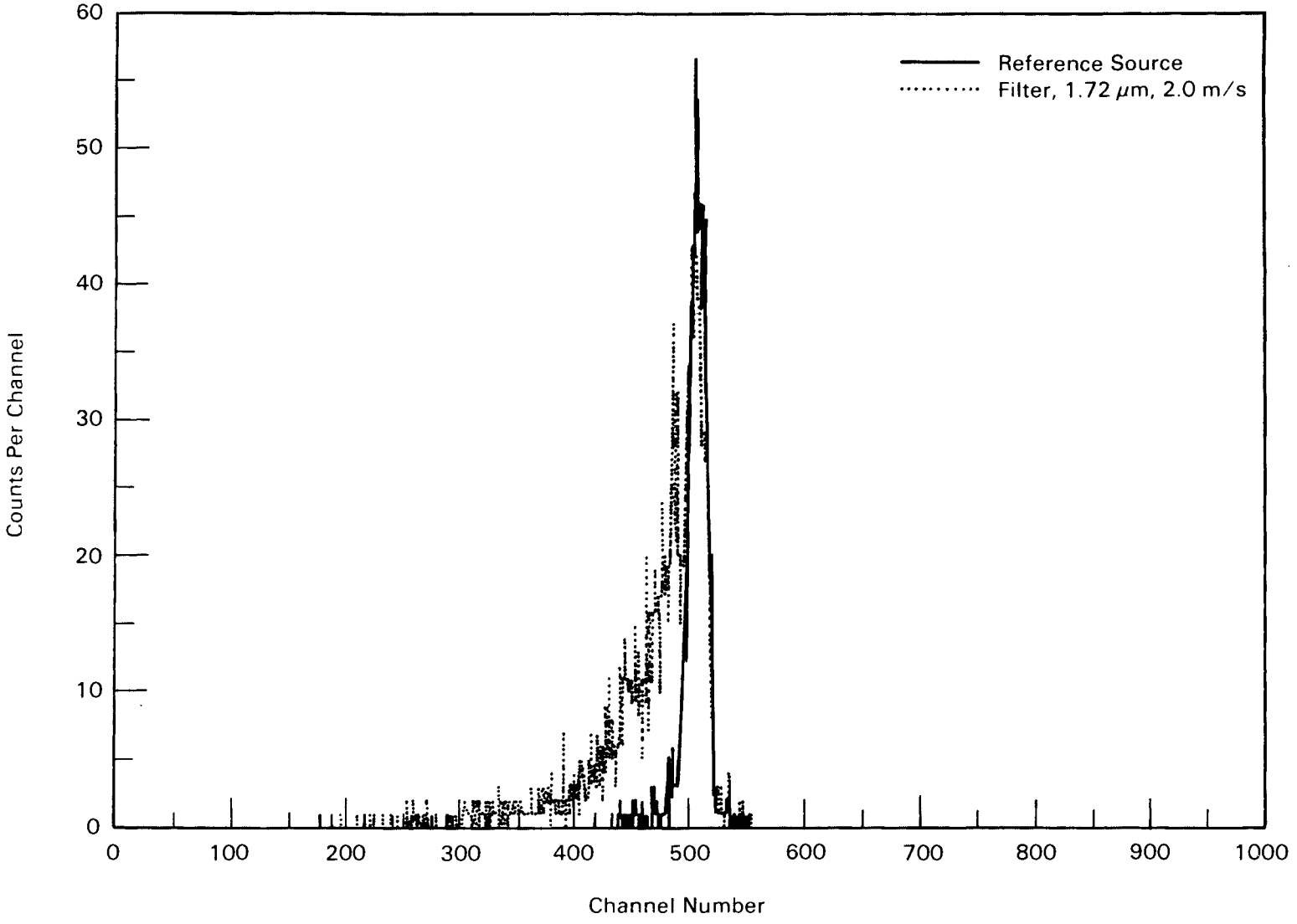

FIGURE 17. Alpha Energy Spectrum of 1.72 μm $^{239}PuO_2$ Deposited on LB-5211 Filter Paper at 2 m/s

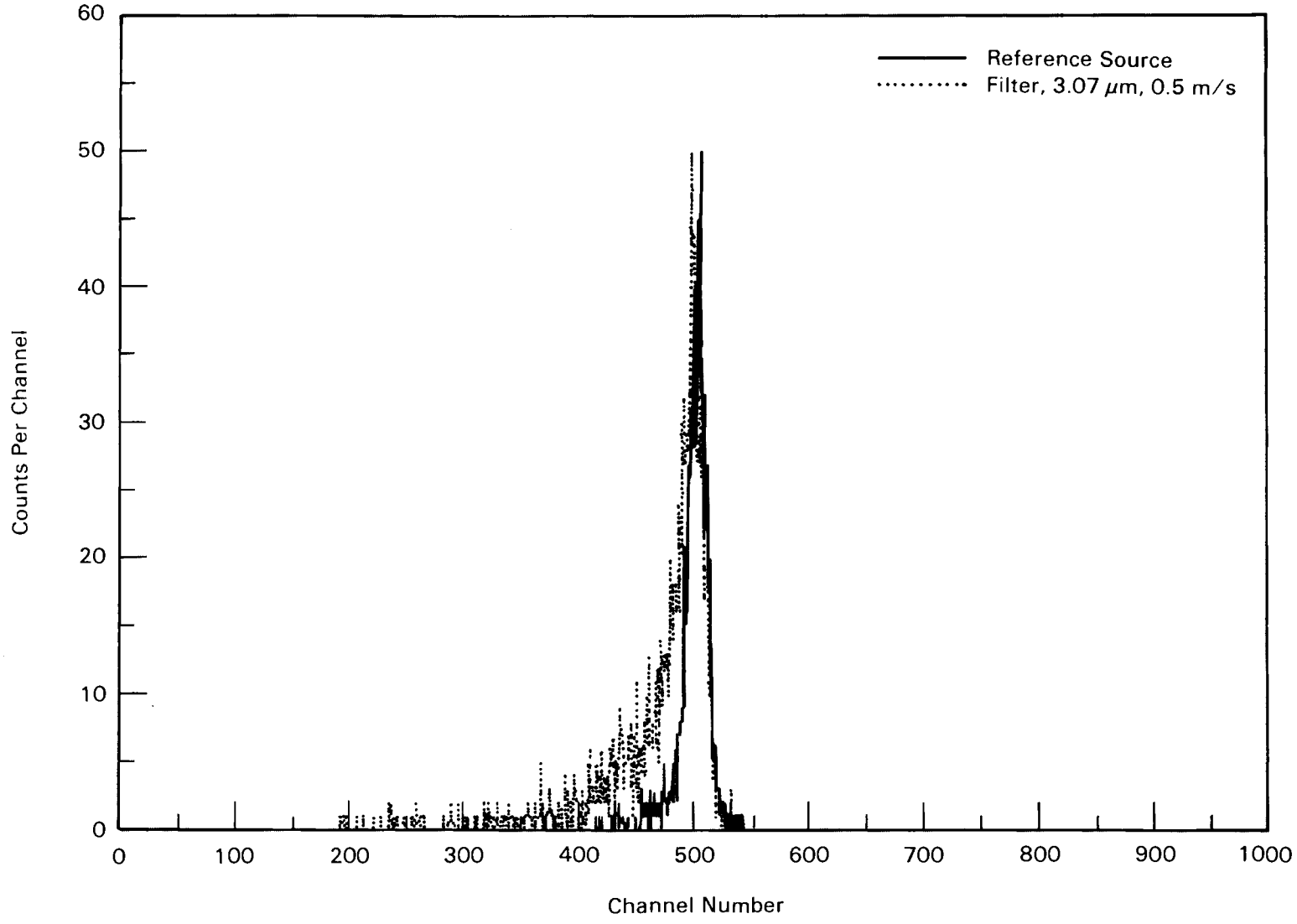

FIGURE 18. Alpha Energy Spectrum of 3.07 μm $^{239}PuO_2$ Deposited on LB-5211 Filter Paper at 0.5 m/s

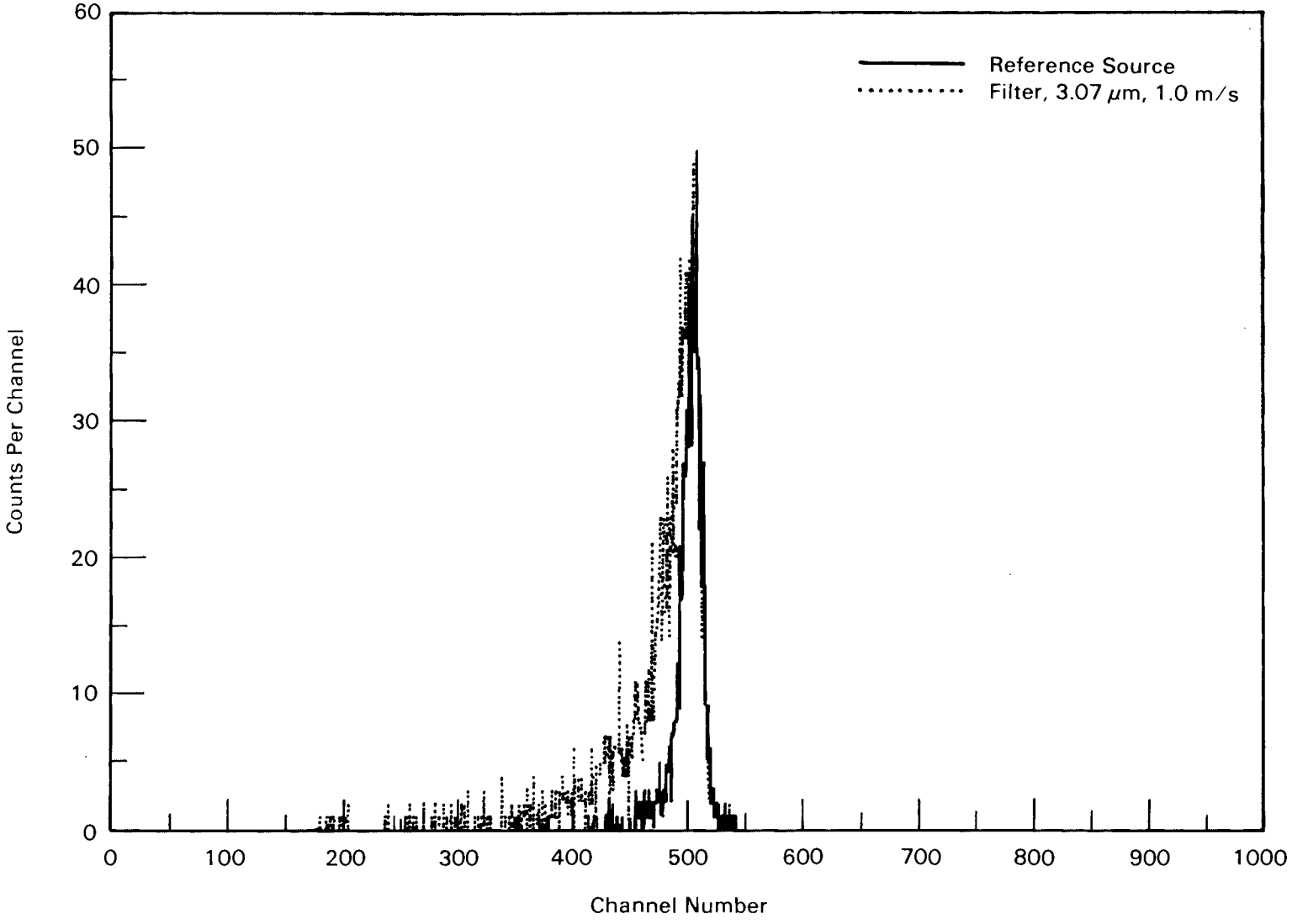

FIGURE 19. Alpha Energy Spectrum of 3.07 μm $^{239}PuO_2$ Deposited on LB-5211 Filter Paper at 1 m/s

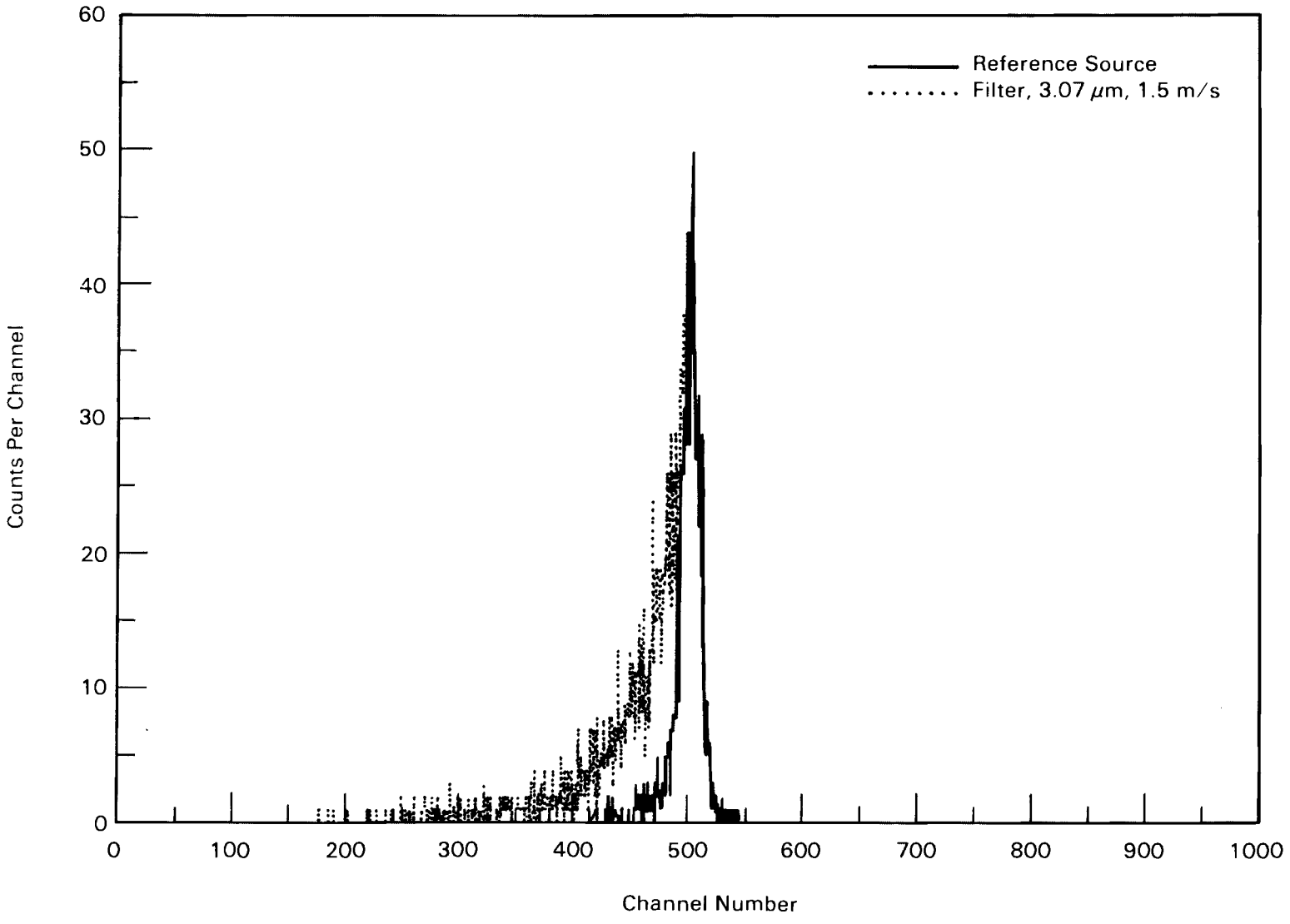

FIGURE 20. Alpha Energy Spectrum at 3.07 μm $^{239}PuO_2$ Deposited on LB-5211 Filter Paper at 1.5 m/s

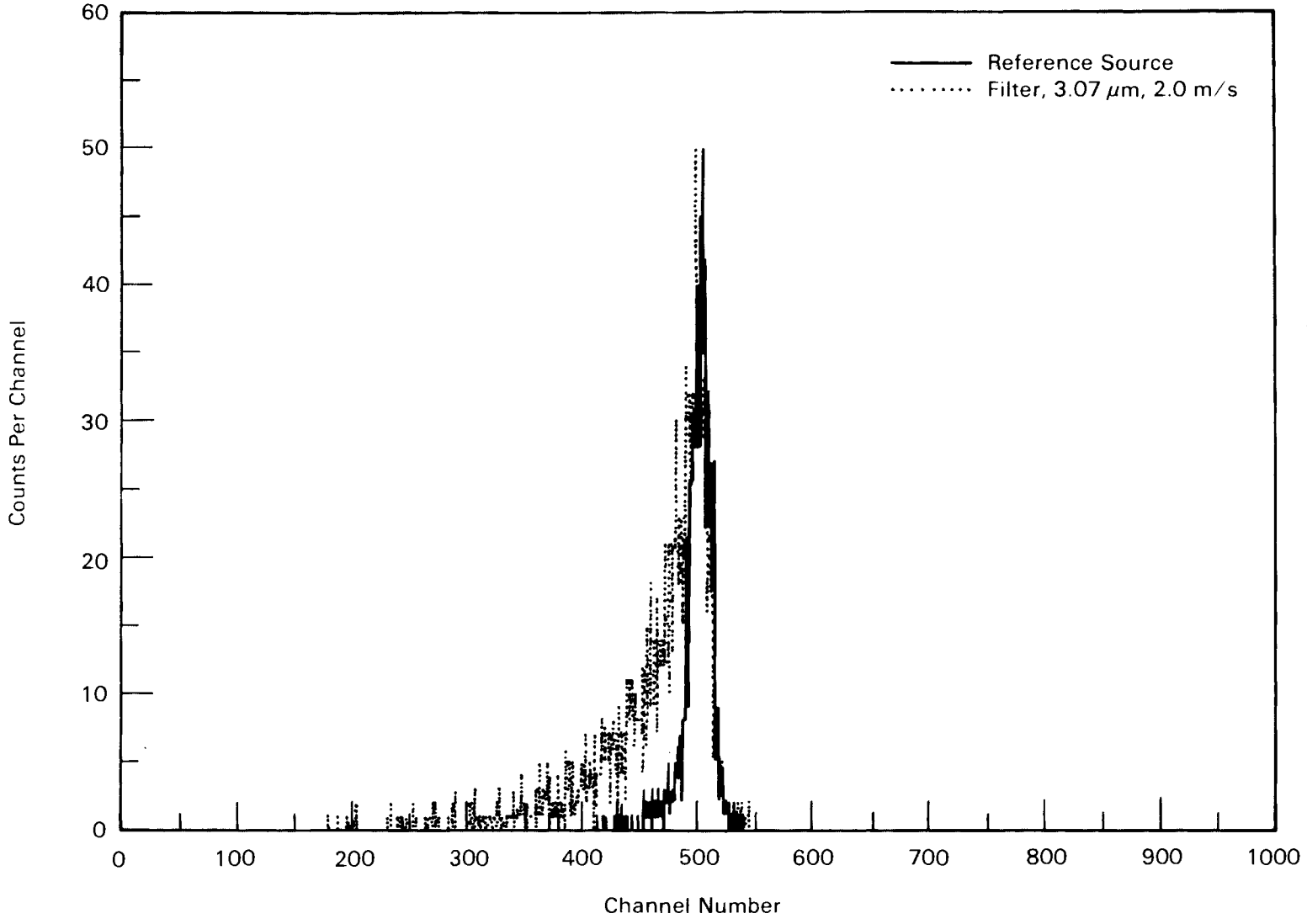

FIGURE 21. Alpha Energy Spectrum of 3.07 μm $^{239}PuO_2$ Deposited on LB-5211 Filter Paper at 2 m/s

Table 11 summarizes the data obtained from direct alpha counting and photon spectrometry of filter samples. In the far right-hand column of the table, activity detected by direct alpha counting is expressed as the fraction of total plutonium (as determined by photon spectrometry). Americium-241 was found to account for less than 1% of the alpha-emitting radioactivity per sample, and was therefore neglected.

The data show significant losses (approximately 15%) due to burial in the filter matrix for the 0.66 μm particle size. The lack of velocity dependence suggests that interception is the dominant collection mechanism, although electrostatic attraction may be significant. This particle size is the closest to the typical most penetrating size for fiber filters (0.1 to 0.3 μm) and this may account for the occurrence of burial losses at all of the velocities tested.

In the case of the 1.72 and 3.07 μm particles, significant burial losses were observed only at 0.5 and 1.0 m/s. This apparent velocity dependence is suggestive of the increasing importance of inertial impaction as particle size increases. As noted in the introduction, inertial impaction is directly dependent on the relaxation time, τ, which is directly dependent on the square of the particle size. Inertial impaction is also dependent on velocity.

A plausible explanation for the lack of significant burial losses at higher velocities for the 1.72 and 3.07 μm particles is that as velocity and particle size increase, the total single fiber efficiency (and thus the overall efficiency) increases because of

TABLE 11. Comparison of Activity Detected by Direct Alpha Count and Photon Spectrometry.

d_a (μm)	Face Velocity (m/s)	ηCi/filter by Alpha Counting	ηCi/filter by Photon Spectrometry	Mean Fraction Detected (f±S.D.)
0.66	0.5	2.54	3.33	
	0.5	4.93	5.83	
	0.5	6.13	6.67	0.84 ± 0.08*
0.66	1.0	5.15	6.17	
	1.0	5.40	5.83	
	1.0	5.22	6.17	0.87 ± 0.05*
0.66	1.5	5.21	6.33	
	1.5	4.87	5.33	
	1.5	4.68	5.67	0.85 ± 0.05*
0.66	2.0	4.25	5.50	
	2.0	4.72	5.17	
	2.0	4.49	5.50	0.83 ± 0.07*
1.72	0.5	2.02	2.17	
	0.5	2.01	2.17	
	0.5	1.93	2.17	0.92 ± 0.02*
1.72	1.0	1.98	1.03	
	1.0	1.02	1.15	
	1.0	0.82	0.98	0.89 ± 0.06*
1.72	1.5	0.59	0.73	
	1.5	0.61	0.67	
	1.5	0.60	0.68	0.84 ± 0.10
1.72	2.0	0.52	0.53	
	2.0	0.48	0.52	
	2.0	0.43	0.50	0.92 ± 0.06
3.07	0.5	2.54	3.00	
	0.5	1.78	2.83	
	0.5	2.04	2.57	0.76 ± 0.11*
3.07	1.0	1.66	1.80	
	1.0	1.47	1.55	
	1.0	1.23	1.34	0.93 ± 0.02*
3.07	1.5	0.96	0.95	
	1.5	1.00	0.92	
	1.5	1.23	1.06	1.03 ± 0.05
3.07	2.0	0.61	0.71	
	2.0	0.66	0.76	
	2.0	0.66	0.68	0.90 ± 0.06

* Indicates rejection of null hypothesis: $f=1$, $P<0.05$.

the additional contribution of inertial impaction. As efficiency increases, there is a tendency for more particles to be collected

earlier as they travel through the filter matrix. Earlier collection means shallower burial and thus decreasing burial losses.

The above data indicate that 0-25% of the alpha-emitting activity collected on filters was collected at some depth greater than the maximum range of the alpha particles. Since most of the alpha-emitting activity is due to ^{239}Pu, the minimum burial depth for an alpha particle to be lost due to absorption is approximately 0.0037 gm/cm^2.

These results are in good agreement with the findings of Stevens and Toureau (1963) in that they confirm that glass-fiber filters tend to be surface collectors, at least at larger particle sizes. However, several important differences exist between the work of Stevens and Toureau and the present study. Apart from the use of a different type of glass-fiber filter, Stevens and Toureau utilized a polydisperse aerosol of uranium acetate. Their particle size was reported as 4.5 μ (mass median diameter) with a geometric standard deviation of 1.6. This represents a wide distribution of particle sizes in which most of the activity is associated with particles > 4.5 μ. The present study dealt with particle sizes that were significantly smaller than those used by Stevens and Toureau. Secondly, the face velocity they used during collection of the aerosol on filters was a uniform 0.35 m/s, significantly slower than the velocities used here. Thus, the present study involved conditions which were designed to maximize the effects of particle size and velocity on burial depth in glass-fiber filters.

CONCLUSION

Burial of airborne particles collected on glass-fiber filters, as measured by alpha counting losses, appears to be a weak function of sampling velocity and particle size within the ranges studied. The results suggest that interception is the dominant collection mechanism in glass fiber filters for particles around 0.66 μm with inertial impaction becoming significant as particle size increases. With increasing particle size comes increasing dependence on sampling velocity and corresponding decreasing burial depth. Alpha energy resolution measurements exhibited some degradation of the alpha energy spectrum from ^{239}Pu particles collected on glass-fiber filters. Loss of resolution was on the order of 2%.

The results demonstrate that absorption of alpha radiation emitted from airborne particles collected on glass-fiber filters does not constitute a major source of error in estimating concentrations of airborne alpha emitting radionuclides. Although the particle size distribution of aerosols sampled under field conditions will rarely be known, the results indicate that a correction which assumes 10 - 15% losses would ensure that concentrations of airborne alpha emitting radionuclides would not be underestimated by collection and analysis on glass-fiber filters.

BIBLIOGRAPHY

Alercio, J. S., and J. H. Harley. 1952. "Evaluation of Alpha-Particle Absorption by Filter Paper." Nucleonics. 10(11):87.

Andersen, B. V. 1963. Particle Size Distribution Found in Air at Hanford Plutonium Fabrication Facilities. HW-SA-3197, Hanford Laboratories, Richland, Washington.

Anscombe, F. J. 1948. "The Transformation of Poisson, Binomial, and Negative Binomial Data." Biometrics. 35:246.

Bichsel, H. 1968. "Charged Particle Interactions." In Fundamentals, Vol I of Radiation Dosimetry, 2nd ed., eds. F. H. Attix and W. C. Roesch, pp. 205-207. Academic Press, New York, New York.

Boback, M. W. 1963. "Absorption of Uranium Alpha Particles by Whatman No. 41 Filter Paper." In Proceedings of the Ninth Annual Conference on Bio-Assay and Analytical Chemistry. TID-7696.

Denham, D. H. 1969. "Effectiveness of Filter Media for Surface Collection of Airborne Radioactive Particulates." In Proceedings of the 3rd Midyear Meeting of the Health Physics Society. p.1093.

Elder, J. C., M. Gonzales, and H. J. Ettinger. 1974. "Plutonium Aerosol Size Characteristics. Health Physics, 27:45.

Freeman, M. F., and J. W. Tukey. 1950. "Transformation Related to the Angular and the Square Root." Annals Math. Stat. 21:607

Hinds, W. C. 1982. Aerosol Technology. E. F. Wiley and Sons, New York, New York.

Hoover, M. D., and W. Stober. 1981. "Model of Particle Deposition in Spinning Duct Aerosol Centrifuges." Aerosol Sciences. J. 12(3):223.

Jonassen, N., and E. I. Hayes. 1974. "A Correction When Measuring ^{222}Rn Daughter Concentration by Alpha Spectroscopy of Filter Samples." Health Physics. 27:310.

Jonassen, N. and E. I. Hayes. 1974. "Absorption of 5.47 MeV Alpha Particles by Membrane Filter Material." Health Physics. 27:313.

Keough, R. F., and G. J. Powers. 1970. "Determination of Plutonium in Biological Materials by Extraction and Liquid Scintillation Counting." Analytical Chemistry. 42(3):419.

Kocher, D. C. 1981. Radioactive Decay Data Tables. pp. 208-211. DOE/TC-11026, National Technical Information Center, Oak Ridge, Tennessee.

Kotrappa, P. and M. E. Light. 1972. "Design and Performance of the Lovelace Aerosol Particle Separation." The Review of Scientific Instruments. 43(8):1106.

Kotrappa, P., and O. R. Moss. 1971. "Production of Relatively Monodisperse Aerosols for Inhalation Experiments by Aerosol Centrifugation." Health Physics. 21:531

Kotrappa, P., C. J. Wilkinson, and H. A. Boyd. 1972. "Technology for the Production of Monodisperse Aerosols of Oxides of Transuranic Elements for Inhalation Experiments." Health Physics. 22:837.

Lee, K. W., and B. Y. H. Lui. 1980. "On the Minimum Efficiency and the Most Penetrating Particle Size for Fibrous Filters." Air Pollution Control Association. J. 30(4):377.

Lindeken, C. L., and W. A. Phillips. 1963. Maximum Burial Depth of Airborne Particles Collected on Membrane Filters. UCRL-7571, p. 19.

Lindeken, C. L., F. K. Petrock, W. A. Phillips, and R. D. Taylor. 1964. "Surface Collection Efficiency of Large-Pore Membrane Filters." Health Physics. 10:495.

Lioy, P. J., et al. 1983. "Air Sampling Instruments for Evaluation of Atmospheric Contaminants." American Conference of Governmental Industrial Hygienists. Sixth edition.

Masters, A. 1983. Personal communications. Mannville Corporation, Denver, Colorado.

Mayneord, W. V., and C. R. Hill. 1969. "Natural and Man-Made Background Radiation." In: Sources, Fields, Measurements, and Applications. Vol. 3 of Radiation Dosimetry. 2nd ed. Eds. F. H. Attix and E. Tochilin, pp 437-438. Academic Press, New York, New York.

Mishima, J. and L. C. Schwendiman. 1972. "Characterization of Radio-active Particles in a Plutonium Plant Exhaust System." In: Pacific Northwest Laboratory Report for 1971 to the USAEC Division of Biology and Medicine, Volume II: Physical Sciences, Part I. Atmospheric Sciences. BNWL-1651, Pt.1, Pacific Northwest Laboratory, Richland, Washington.

Parnianpour, H. 1967. Study of the Penetration of Aerosols into Filter Beds. ANL-TRANS 655.

Raabe, O. G., et al. 1975. "Development and Use of a System for Routine Production of Monodisperse Particles of $^{238}PuO_2$ and Evaluation of Gamma Emitting Labels." Health Physics. 28:655.

Sherwood, R. J. and D. C. Stevens. 1965. "Some Observation on the Nature and Particle Size of Airborne Plutonium in the Radiochemical Laboratories of Harwell." Ann. Occup. Hyg. 8:93.

Simons, J. G. 1956. A Correction For the Absorption of Plutonium Alpha Particles in Filter Paper Used for Dust Sampling. AERE. HP/M 87.

Stafford, R. G., and H. J. Ettinger. 1972. "Filter Efficiency as a Function of Particle Size and Velocity." Atmospheric-Environment. 6:353.

Stevens, D. C., and Toureau, A. E. R. 1963. The Effect of Particle Size and Dust Loading on the Shape of Alpha Pulse Height Spectra of Air Sample Filters. AERE-R 4249.

Stober, W., and H. Flachsbart. 1969. Size-Separating Precipitation of Aerosols in a Spinning Spiral Duct. UR-49-1060.

Velleman, P. F. 1980. "Definition and Comparison of Robust Nonlinear Data Smoothing Algorithms." J. Am. Stat. Assoc. 75(371):609.

DISTRIBUTION

No. of Copies

OFFSITE

27 Technical Information Center

DOE Headquarters

R. W. Barber, Acting Director
Nuclear Reactor and Facility Safety Division, PE-221
U. S. Department of Energy
Washington, D. C. 20545

S. T. Brewer
Assistant Secretary for
Nuclear Energy, NE-1
U. S. Department of Energy
Washington, D. C. 20545

B. P. Brown, Leader
Process Facilities Safety, EP-341
U. S. Department of Energy
Washington, D. C. 20545

G. L. Chipman, Jr.
Deputy Assistant Secretary
Breeder Reactor Programs, NE-50
U. S. Department of Energy
Washington, D. C. 20545

J. W. Culpepper, Deputy Asst. Sec.
Security Affairs, DP-30
U. S. Department of Energy
Washington, D. C. 20545

L. J. Deal, Acting Director
Division of Radiological Controls, PE-222
U. S. Department of Energy
Washington, D. C. 20545

L. A. Forsythe, Deputy Director
Safety Environment and Emergency Actions, DP-226
U. S. Department of Energy
Washington, D. C. 20545

No. of Copies

N. Goldenberg, Director
Safety QA and Safeguards, NE-74
U. S. Department of Energy
Washington, D. C. 20545

Major General W. W. Hoover, USAF
Deputy Assistant Secretary for
Military Application, DP-20
U. S. Department of Energy
Washington, D. C. 20545

B. R. House, Deputy Asst. Sec.
Energy Emergencies, EP-40
U. S. Department of Energy
Washington, D. C. 20545

A. G. Joseph, Director
Office of Field Operations Management, ER-40
U. S. Department of Energy
Washington, D. C. 20545

K. O. Laughon, Sr., Director
Office of Spent Fuel Management and Reprocessing Systems, NE-40
U. S. Department of Energy
Washington, D. C. 20545

J. R. Maher, Director
Nuclear Safety Office, PE-22
U. S. Department of Energy
Washington, D. C. 20545

J. W. Mares, Asst. Secretary
Policy, Safety, & Environment, EP-1
U. S. Department of Energy
Washington, D. C. 20545

S. Matovich, Director
Safety & Quality Assurance Staff
Nuclear Materials Prod, DP-13
U. S. Department of Energy
Washington, D. C. 20545

No. of Copies

Admiral K. R. McKee
Deputy Assistant Secretary for Naval Reactors, NE-60
U. S. Department of Energy
Washington, D. C. 20545

W. E. Mott, Technical Assistant
Office of Operational Safety, EP-323
U. S. Department of Energy
Washington, D. C. 20545

M. P. Norin
Office of Support & Programs, NE-74
U. S. Department of Energy
Washington, D. C. 20545

D. E. Patterson, Director
Office of Operational Safety, PE-24
U. S. Department of Energy
Washington, D. C. 20545

B. Siebert, Director
Policy, Planning, and Coordination Staff, DP-31
U. S. Department of Energy
Washington, D. C. 20545

R. J. Stern, Director
Environmental Compliance, EP-36
U. S. Department of Energy
Washington, D. C. 20545

L. E. Temple, Director
Construction Management, ER-65
U. S. Department of Energy
Washington, D. C. 20545

J. W. Thiessen, Deputy Assoc. Dir.
Office of Health & Environmental Research, ER-71
U. S. Department of Energy
Washington, D. C. 20545

No. of Copies

R. E. Tiller, Acting Deputy Assistant Secretary
Environment, Safety, and Health, PE-20
U.S. Department of Energy
Washington, D.C. 20545

A. W. Trivelpiece, Director
Office of Energy Research, ER-1
U. S. Department of Energy
Washington, D. C. 20545

25 E. J. Vallario, Manager
Health Physics
Radiological Controls Div., EP-342
U. S. Department of Energy
Washington, D. C. 20545

DOE Albuquerque Operatons Office

R. E. Alexander, Safety Director
Pantex Plant
Mason & Hanger--Silas Mason Co., Inc.
P. O. Box 30020
Amarillo, TX 79177

W. D. Burnett, Manager
Health Physics Division
DOE Sandia National Laboratories
Mail Code 3312, Bldg. 8619
P. O. Box 2800
Albuquerque, NM 87115

J. E. Dummer, Group Leader
Health Physics
Los Alamos National Laboratory
P. O. Box 1663
Los Alamos, NM 87545

E. P. Forest, Manager
Environmental Health & Safety
Neutron Devices Department
General Electric Company
P. O. Box 11508
St. Petersburg, FL 33733

No. of Copies

H. E. Meyer, Manager
Health Physics
Mound Laboratory
Monsanto Research Corporation
P. O. Box 32
Miamisburgn, OH 45342

P. M. Ramey
Albuquerque Operations Office
U. S. Department of Energy
P. O. Box 5400
Albuquerque, NM 87115

J. J. Thompson
Lovelace Biomedical & Environmental Research Laboratories
Health Protection Operations
P. O. Box 5890
Alburquerque, NM 87115

R. E. Yoder, Director
Health, Safety, and Environment
Rockwell International
P. O. Box 888
Golden, CO 80401

DOE Chicago Operations Office

L. V. Coulson, Head
Safety Section
Fermi National Accelerator Laboratory
P. O. Box 500
Batavia, IL 60510

C. B. Meinhold, Head
Safety & Environmental Protection Division
Brookhaven National Laboratory
Associated Universities, Inc.
Upton, NY 11973

R. Moser, Director
Operational & Environmental Safety Division
Chicago Operations Office
U. S. Department of Energy
9800 South Cass Avenue
Argonne, IL 60439

No. of Copies

D. A. Waite
Battelle Columbus Laboratories
505 King Street
Columbus, OH 43201

DOE Idaho Operations Office

J. H. Barry, Director
Operational Safety Division
Idaho Operations Office
U. S. Department of Energy
550 2nd Street
Idaho Falls, ID 83401

B. J. Beers, Assistant Manager
Environmental, Safety and Health Programs
Idaho Operations Office
U. S. Department of Energy
550 2nd Street
Idaho Falls, ID 83401

B. L. Rich
Health and Safety Division
EG&G Idaho
P.O. Box 1625
Idaho Falls, ID 83401

DOE Naval Reactors Office

A. C. Davis, Manager
Bettis Atomic Power Lab. (DOE)
Westinghouse Electric Corporation
P. O. Box 79
West Mifflin, PA 15122

T. L. Collins, Manager
Knolls Atomic Power Laboratory
U. S. Department of Energy
P. O. Box 1072
Schenectady, NY 12301

C. K. Gaddis, Manager
Pittsburgh Naval Reactors Office
P. O. Box 109
W. Mifflin, PA 15122

No. of
Copies

DOE Nevada Operations Office

A. E. Bicker
Reynolds Electrical & Engineering Co., Inc.
P. O. Box 14400
Las Vega, NV 89114

B. W. Church
Health Physics Division
Nevada Operations Office
U. S. Department of Energy
P. O. Box 14100
Las Vegas, NV 89114

S. R. Elliot, Director
Office of Safety and Health
Nevada Operations Office
U. S. Department of Energy
P. O. Box 14100
Las Vegas, NV 89114

DOE Oak Ridge Operations Office

M. W. Boback, Director
Health and Safety
National Lead Company of Ohio
P. O. Box 39158
Cincinnati, OH 45239

W. R. Golliher, Manager
Health, Safety and Environmental Affairs
Oak Ridge Gaseous Diffusion Plant
P. O. Box P
Oak Ridge, TN 37831

C. M. Hutchings, Administrator
Medical, Safety, and Environment
Goodyear Atomic Corporation
P. O. Box 628
Piketon, OH 45661

J. B. McLendon, Director
Radiation Safety, Y-12
Nuclear Division
Union Carbide Corporation
P. O. Box Y
Oak Ridge, TN 37830

No. of
Copies

D. C. Parzyck, Director
Environmental and Occupational Safety Division
Oak Ridge National Laboratory
P. O. Box X
Oak Ridge, TN 37830

W. E. Thompson
Health, Safety, and Environmental Control
Paducah Gaseous Diffusion Plant
P.O. Box 1410
Paducah, KY 42001

W. H. Travis, Director
Safety & Environmental Control Division
Oak Ridge Operations Office
U. S. Department of Energy
P. O. Box E
Oak Ridge, TN 37830

J. C. White, Manager
Technical Services
Nuclear Division
Union Carbide Corporation
Oak Ridge, TN 37830

DOE San Francisco Operations Office

J. T. Davis, Chief
Operational Safety and Compliance
San Francisco Operations Office
U. S. Department of Energy
1333 Broadway
Oakland, CA 94612

W. E. Keheley, Branch Chief
Environment and Nuclear Safety
San Francisco Operations Office
U. S. Department of Energy
1333 Broadway (Wells Fargo Bldg)
Oakland, CA 94612

No. of Copies

R. C. McCall, Rad. Safety Officer
Stanford Linear Accelerator
P. O. Box 4349
Stanford, CA 94305

R. H. Thomas
DOE Lawrence Berkeley National Laboratory
University of California
Berkeley, CA 94720

A. J. Toy, Head
Hazardous Control Department
Lawrence Livermore National Lab.
P. O. Box 808
Livermore, CA 94550

DOE Savannah River Operations Office

W. A. Reese, Director
Safety and Environmental Division
Savannah River Operations Office
U. S. Department of Energy
P. O. Box A
Aiken, SC 29801

W. C. Reining, Superintendent
Health Protection Department
E.I. DuPont De Nemours and Company
Savannah River Plant
Aiken, SC 29809

M. J. Sires III, Assistant Manager
Health Safety and Environment
Savannah River Operations Office
U. S. Department of Energy
P. O. Box A
Aiken, SC 29801

EPA Office of Radiation Programs

A. Richardson
Criteria & Standards Division, AW-460
401 M Street, SW
Washington, D. C. 20460

No. of Copies

National Center for Devices and Radiological Health

J. C. Villforth, Director
FDA Bureau of Radiological Health
Rockville, MD 20852

Nuclear Regulatory Commission

R. E. Alexander, Chief
Occupational Radiation Branch
Office of Nuclear Regulatory Research
Nuclear Regulatory Commission
Washington, D.C. 20555

R. E. Minogue, Director
Office of Nuclear Regulatory Research
Nuclear Regulatory Commission
Washington, D. C. 20555

D. Muller, Assistant Director
Environmental Technology
Office of Nuclear Reactor Regulation
Nuclear Regulatory Commission
Washington, D. C. 20555

L. C. Rouse, Chief
Advanced Fuel and Spent Fuel Licensing Branch
Division of Fuel Cycle & Material Safety
Nuclear Regulatory Commission
Washington, D. C. 20555

No. of Copies

ONSITE

4 DOE Richland Operations Office

P. K. Clark/H. E. Ransom
D. R. Elle
R. E. Gerton
G. R. Yesberger

2 Rockwell - Hanford

B. E. Knight
B. J. Saueressig

1 Hanford Environmental Health Foundation

R. D. Gilmore

3 UNC Nuclear Industries

D. F. Brendel
W. L. Ness
D. J. Pisarcik

4 Westinghouse Hanford Co.

R. O. Budd
G. D. Carpenter
W. P. Howell
R. L. Watts

No. of Copies

46 Pacific Northwest Laboratory

J. R. Berry
P. E. Bramson
L. C. Carrick
R. L. Dirkes
J. T. Denovan
L. G. Faust
W. M. Fleming
D. P. Higby (20)
J. L. Kenoyer
H. V. Larson
A. P. Mileham
B. L. Murphy
N. P. Nisick
K. R. Price
J. M. Selby (5)
K. L. Swinth
Publishing Coordination (2)
Technical Information (5)